Approved for public release; distribution is unlimited.

Science Plan

Sea State and Boundary Layer Physics of the Emerging Arctic Ocean

by J. Thomson[1], V. Squire[2], S. Ackley[3], E. Rogers[4], A. Babanin[5], P. Guest[6], T. Maksym[7], P. Wadhams[8], S. Stammerjohn[9], C. Fairall[9], O. Persson[9], M. Doble[10], H. Graber[11], H. Shen[12], J. Gemmrich[13], S. Lehner[14], B. Holt[15], T. Williams[16], M. Meylan[17], and J. Bidlot[18]

[1] *Applied Physics Laboratory, University of Washington*
[2] *University of Otago*
[3] *University of Texas at San Antonio*
[4] *Naval Research Laboratory, Stennis*
[5] *Swinburne University of Technology*
[6] *Naval Postgraduate School*
[7] *Woods Hole Oceanographic Institution*
[8] *Cambridge University*
[9] *University of Colorado, Boulder*
[10] *Laboratoire d'Oceanographie de Villefranche*
[11] *University of Miami*
[12] *Clarkson University*
[13] *University of Victoria*
[14] *German Aerospace Center (DLR)*
[15] *Jet Propulsion Laboratory*
[16] *Nansen Environmental and Remote Sensing Center*
[17] *University of Newcastle*
[18] *European Centre for Medium-Range Weather Forecasts*

Technical Report

APL-UW 1306

September 2013

Applied Physics Laboratory University of Washington
1013 NE 40th Street Seattle, Washington 98105-6698

Grant numbers: Ackley, N000141310435; Babanin, N000141310278; Doble, N000141310290; Fairall, N0001413IP20046; Gemmrich, N000141310280; Graber, N000141310288; Guest, N0001413WX20830; Holt, N0001413IP20050; Lehner, N000141310303; Maksym, N000141310446; Rogers, N0001413WX20825; Shen, N000141310294; Squire, N000141310279; Stammerjohn, N000141310434; Thomson, N000141310284; Wadhams, N000141310289

Acknowledgments

The authors thank Office of Naval Research Program Managers Martin Jeffries and Scott Harper for initiating the program and supporting research in the emerging arctic.

Contents

1 Executive Summary

The Office of Naval Research initiated a Department Research Initiative (DRI) titled *Sea State and Boundary Layer Physics of the Emerging Arctic Ocean*. The central hypothesis of the 'Sea State' DRI is that surface waves now have a much greater role in the contemporary Arctic Ocean. Indeed, the entire Arctic Ocean in summer may soon resemble a marginal ice zone (MIZ), where waves propagate through the ice pack and affect the evolution of sea ice over large scales. This large-scale pattern feeds back, as wave generation is controlled by the amount of open water fetch. At smaller scales, waves and ice interact to attenuate and scatter the waves while simultaneously fracturing ice into ever changing floe size and thickness distributions. Further complicating these processes are forcing by winds and surface fluxes from the ocean to the atmosphere, which are expected to increase with heightened storm activity in the region. The marginal open seas provide new opportunities and new problems. Navigation and other maritime activities become possible, but waves, storm surges and coastal erosion will likely increase. Air–sea interactions enter a completely new regime, with momentum, energy, heat, gas, and moisture fluxes being moderated or produced by the waves, and impacting upper-ocean mixing.

The Sea State DRI will use a combination of modeling, in situ observations, and remote sensing to address the following science objectives:

- Develop a sea state climatology for the Arctic Ocean
- Improve wave forecasting in the presence of sea ice
- Improve theory of wave attenuation/scattering in the sea ice cover
- Apply wave–ice interactions directly in integrated arctic system models
- Understand heat and mass fluxes in the air–sea–ice system

The DRI will focus on arctic conditions during the late summer and early autumn, especially the freeze-up of the Beaufort and Chukchi seas, to capture the strongest storms and maximum open water. This focus also complements the Marginal Ice Zone DRI (MIZ-DRI) that is studying the summer breakup and ice retreat. Field observations will be collected primarily during a cruise in the fall of 2015, supplemented by long-term moorings and autonomous platforms.

This *Science Plan* presents the overall goals and approach of the Sea State DRI. Individual contributions are noted, but the focus is on an integrated vision of the science. Although many of the details will necessarily evolve during the five-year program (2013–2017), it is expected that the priorities defined herein will continue to guide the science that is carried out.

2 Introduction

2.1 The emerging Arctic Ocean

The Arctic Ocean is rapidly evolving, particularly at the surface, where air, sea, and ice interact to exchange heat and momentum. Compared with earlier decades, arctic sea ice cover has thinned, shifted from predominantly perennial ice to seasonal ice, and has reduced in extent to nearly 30% less at the end of the summer melt period (Meier et al., 2013). Other indications of significant change include increased sea ice deformation relating to the thinning ice (Rampal et al., 2009), increased ocean primary productivity (Arrigo and van Dijken, 2011; Arrigo et al., 2012), shifts in the marine ecosystem (Grebmeier et al., 2006) and longer periods of summer ice melt (Markus et al., 2009). In concert with the decline in the sea ice cover, shifts in arctic atmospheric circulation are occurring (Overland et al., 2012) along with changes to global weather patterns in the Northern Hemisphere (Francis et al., 2009; Dobrynin et al., 2012). The possibility of an ice-free summer during the first half of the 21st century has been designated highly probable (e.g., Overland and Wang, 2013). It is likely that the reduced ice cover is associated with recent storm activity, such as occurred during the great cyclone in August 2012 (Simmonds and Rudeva, 2012; Zhang et al., 2013; Parkinson and Comiso, 2013). The expectation is that severe storms will occur more often, and that the combination of stronger winds and increased fetches of open water will produce larger waves throughout the region (Francis and Vavrus , 2012; Francis et al., 2011; Asplin et al., 2012; Vermaire et al., 2013).

As an example of wave-enhanced destruction of sea ice, an unusually strong storm formed over Siberia on 5 August 2012 and moved over the central Arctic causing dispersion and separation of a significant amount of preconditioned sea ice (Figure 1) (Parkinson and Comiso, 2013). As a result, the interior pack became more exposed to wind and waves associated with the cyclone, facilitating the further sea ice decay observed. The cyclone reduced the minimum September ice extent by almost 200,000 square kilometers, an additional five percent. This is part of a larger pattern of stronger autumn storms in recent years (Serreze et al., 1993, 2001; Zhang et al., 2004), which coincides with increased open water and enhanced air–sea fluxes of heat and momentum, particularly in the Beaufort and Chukchi seas (Kwok and Untersteiner, 2011; Simmonds and Keay, 2009; Stroeve et al., 2005, 2008).

A hindcast of the wave heights during the cyclone of August 2012 predicts waves as great as 5 m in the region of maximum ice loss (Figure 2). Although global wave models at all major operational centers include at least a portion of the Arctic, lack of in situ data has prevented any ground truth validation of the model output. Clearly, large waves are present and a changing wave regime may be further enhancing the ice retreat through increased melt rates, acting as an additional positive influence on ice albedo–temperature feedback. Indeed,

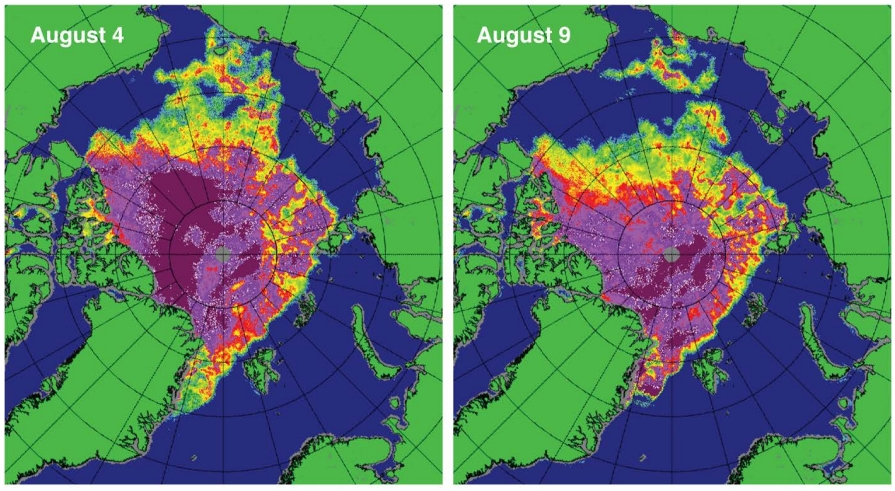

Figure 1: Maps of sea ice concentration from the SSMIS showing the rapid loss of ice in the Beaufort and Chukchi seas during the great arctic cyclone of August 2012. Magenta and purple colors indicate ice concentration near 100%; yellow, green, and pale blue indicate 60% to 20% ice concentration. On three consecutive days (August 7, 8, and 9), sea ice extent was reduced by nearly 200,000 square kilometers. Image: National Snow and Ice Data Center, courtesy IUP Bremen.

statistically significant larger positive trends in extreme wave heights are occurring at high latitudes, generated by local storm events correlated with stronger winds (Young et al., 2011). Francis et al. (2011) corroborate this for the Arctic in particular.

By breaking up the sea ice, the incident ocean waves cause the sea ice to act like a marginal ice zone (MIZ). Penetrating wave trains help it to melt more easily (Wadhams et al., 1979; Steele et al., 1989; Gladstone et al., 2001) and to become more compliant, boosting their ability to destroy more of the enervated sea ice mass that remains, and producing a less compact and hence more dynamic ice field. The resulting proliferation of open water also promotes further melting and further wave growth, as amassed fetch is increased. In the winter, on the other hand, breakup by waves can enhance ice growth by creating openings that freeze over rapidly. In both cases, the new floe size distribution (FSD) and arrangement of open water and sea ice created affect air–sea exchanges directly.

In the MIZ, surface waves are normally the main agent responsible for ice fragmentation and, depending upon wave and sea ice properties, can propagate long distances into the ice field and contribute to fracture. Indeed, Prinsenberg and Peterson (2011) recorded flexural failure induced by swell propagating within multiyear pack ice during the summer of 2009, *even* at very large distances (> 100 km) from the ice edge in the Beaufort Sea. While the ice observed in the Beaufort Sea qualified as being preconditioned, namely heavily decayed by melting (Barber et al., 2009) and thus more fragile, these observations suggest that such

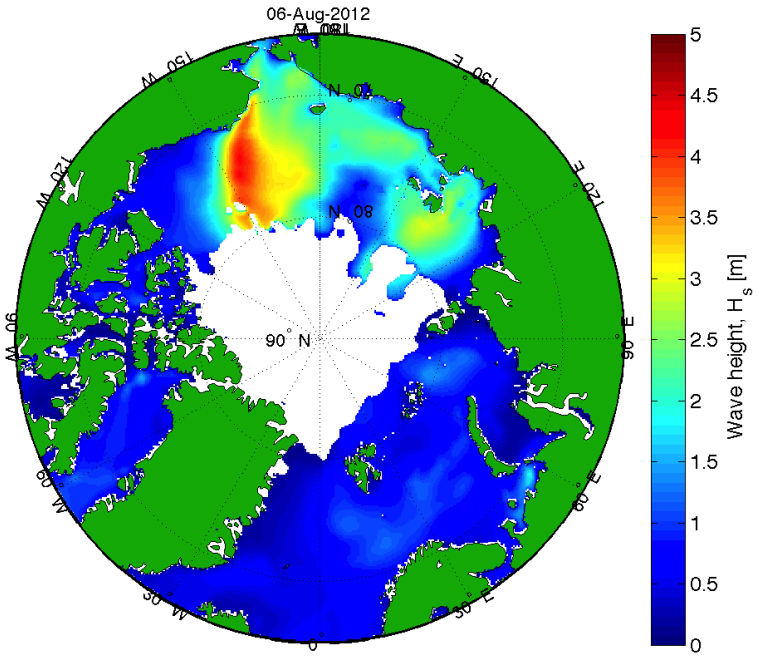

Figure 2: Significant wave heights (in meters) from a WAVEWATCH III hindcast of the August 2012 arctic cyclone, showing large waves in the Beaufort and Chukchi seas coincident with a dramatic loss of sea ice. Image: E. Rogers and J. Thomson (unpublished).

events could occur more frequently deep within the ice pack in a warmer Arctic (i.e., one that is no longer protected by a durable, extensive shield of sea ice).

Some future ice advance and ice growth scenarios in the Arctic are:

i. Typical ice advance. New ice formation takes place as thin sheets evolving into first year ice primarily through congelation growth. Although snowfall occurs in fall, the net snow accumulation is similar to years past (Warren et al., 1998; Kwok and Cunningham, 2008); thus, despite the delayed sea ice growth season, winter first year ice thickness will be comparable to what has been observed in recent years, i.e., 1.5 to 1.8 m [based on modeling, e.g., see PIOMAS results[1]; airborne observations by EMI (Haas, 2012) and NASA Operation IceBridge[2]; and satellite observations, e.g., IceSAT (Kwok, 2009) and CryoSat]. Additional ocean heat added during the extended summer open water period is removed from the mixed layer during autumn cooling and mixing. While 2012 presented a new all-time summer minimum (3.7 million square km), the last six years have not decreased steadily but have

[1] `http://www.nsidc.org`

[2] `http://www.nasa.gov/mission_pages/icebridge/index.html`

fluctuated around a higher mean area ($\sim 4.6 \pm 0.25$ million square km). This scenario suggests, if thickness has not changed during this period, a possible equilibrium could be reached with arctic summer sea ice remaining at/around this level until driven lower by external events, e.g., increased transport of sea ice out of the Arctic as observed in 2007, or enhanced breakup and melting such as occurred during the extended storm of August 2012. Measurements following the initial fall growth are also needed to resolve how winter ice thickness may (or may not) be changing, especially given the uncertainty in model calculations (PIOMAS), and airborne (IceBridge) and satellite measurements (CryoSAT).

ii. Typical ice advance, but with winter effects of stored ocean heat. If not all the ocean heat is removed prior to, or during, the initial ice growth (Jackson et al., 2012; Steele et al., 2011), the additional heat may be released gradually. This will increase the ocean heat flux at the ice–ocean boundary, where formerly it was approximately $0\,\mathrm{W}^{-2}$. If this ocean heat is of the order 5–7 $\mathrm{W\,m}^{-2}$, studies from the Antarctic (Lytle and Ackley, 1996; Lewis et al., 2011) suggest that the upper limit of thermodynamic ice growth may drop to 1.1 to 1.4 m by end of winter. Thinner ice is prone to more extensive melt ponds (Polashenski , 2012), causing an earlier sea ice retreat and melt the following summer, and could lead to a more delayed advance (Stammerjohn et al., 2012) the following fall. If winter stored ocean heat remained and resulted in even higher winter ocean heat flux, this process could further drive summer ice extent toward ice-free summer conditions.

iii. An Antarctic-like ice edge. With increased open water during summer–fall, there is a propensity for wave fields to develop and increase (in duration and/or magnitude) during storms, concurrent with falling air temperatures during the transition from summer to fall. In the Antarctic, the wave field results in both increased turbulence in the water and rapid ice growth as a frazil-pancake ice cycle develops (Lange et al., 1989). The initial growth of pancake ice, however, causes a negative feedback to the waves; the waves decay, pancake growth ceases and an intact ice cover soon develops. If ocean heat has been exhausted prior to, or during, the initial ice growth, thermodynamic growth (columnar ice) then continues, similar to scenario (i) without further pancake ice formation. Net seasonal ice thickness may still be controlled primarily by temperatures throughout the winter period, and although initial thickness may be higher, the net thickness will still be controlled by thermodynamic growth and reach levels as in (i) (1.5 to 1.8 m). The default for a net effect on future ice loss in the Arctic may therefore be similar to (i), a tendency toward a stable environment at the 'new-normal' unless triggered by an external event. There may be a further complication if stored ocean heat (ii) is also involved, although the increase in storms and wave action, as well as affecting the ice formation mode, may also be efficient in removing stored ocean heat prior to initial ice formation.

2.2 Motivation and naval relevance

It has been proposed that the dramatically reduced ice cover in the Arctic will lead to increased vessel traffic and use of maritime resources (Showstack, 2013; Stephenson et al., 2011). Safe and secure operations in the Arctic will require high-precision forecasts of weather, sea state, and sea ice. Improved spatial resolution has significantly enhanced how models represent the mean sea state and its variability, but it has also highlighted a number of problems that have remained hidden. The absence of wave–ice interactions in modern models is a significant deficiency of major importance to all maritime endeavors in the Arctic.

In addition to the urgent need for advanced forecasting via improved model physics, the time is ripe for new observations of wave–ice mechanics and flux. The last major field efforts in these areas were the Marginal Ice Zone Experiments (MIZEX) in 1984–1987 and the Surface Heat Budget of the Arctic Ocean (SHEBA) project in 1997. In the intervening decades, technology has changed dramatically. For example, motion sensors enabling directional wave resolution by buoys are now readily available and inexpensive (Herbers et al., 2012), and the data can be telemetered in real time globally. Similarly, direct flux measurements from shipboard systems now remove ship motions reliably, even during high sea states. Furthermore, satellite remote sensing products now make it possible to observe spatial variability across a wide range of scales. Finally, computational resources are now sufficient to assimilate in situ data and satellite products into complex system models with detailed physics. Thus, the present Sea State DRI is poised to contribute major advances in understanding key processes of the emerging Arctic Ocean and to improve future predictions of sea state and sea ice.

2.3 Sea state and boundary layer processes

In the Arctic Ocean, surface fluxes are influenced by sea state (i.e., waves) and sea ice cover. These fluxes, in turn, increase or reduce the sea ice and thereby set the fetch available to grow waves and determine a sea state. A unique aspect of the Arctic is the variable fetch, which changes with ice cover and may limit or enhance wave growth. In open water, we expect many of the mid-latitude bulk fluxes (e.g., Fairall et al., 2003) to apply, where waves set the ocean surface drag (in response to winds) and radiative fluxes can be strong. In a full ice cover, we expect an ice mass balance and wind forced drag profiles beneath the surface. In a marginal ice zone, these expectations are complicated by strong interactions between waves and ice.

Wave–ice interactions have been a focus of theoretical studies for a long while, as exemplified by early and recent analytical papers (Peters, 1950; Bennetts and Squire, 2012a); the first known study was actually in the nineteenth century (Greenhill, 1887). The fundamental fluid mechanics that undergirds the physics, however, has provided little quantitative guidance

to operational forecasting models in the past, with the result that such models have used speculative parametric treatments without reference to the details of strong theoretical formulations. Recent work (Dumont et al., 2011a; Williams et al., 2013a,b) offers significant promise in this context.

There are several different theories for wave–ice interactions. Rogers et al. (2011) suggests four classes for such theories: viscous (e.g., Newyear and Martin, 1999); viscoelastic (e.g., Wang and Shen, 2010); turbulent (e.g., Liu et al., 1991b); and scattering (Perrie and Hu, 1996; Bennetts and Squire, 2012a). Scattering theories can be further subdivided into scattering by separate ice floes, common in the MIZ, and scattering from irregularities such as cracks, pressure ridges, open and refrozen leads, etc., in the ice canopy when the sea ice is more continuous (Bennetts and Squire, 2012a). To this collection, Wang and Shen (2010) add the mass loading model (Peters, 1950), the thin elastic plate model (Greenhill, 1887, or, e.g., Wadhams , 1973), and floe–floe collisions (Shen and Squire, 1998). Some of these theories are dissipative, others such as the mass-loading model and scattering when the ice is taken to be perfectly (in)elastic are not — noting that the latter models usually also now include viscous dissipation. Therefore, even qualitatively, these groups of theories address different processes—the attenuation of wave energy and the energy-conserving changes to the wave spectrum. Within the energy-conserving theories, the elastic-layer model predicts wave lengthening, whereas the mass-loading model produces wave shortening.

Among such theories, the scattering theory models are the most sophisticated mathematically and they are applicable to the MIZ, which is formed from the breakup of the pack ice.

Amongst other things, reviews of wave–ice interactions by Squire et al. (1995) and Squire (2007) clarify the decrease in wave amplitude caused by ice covers. Near the ice margin (i.e., the boundary between the open ocean and the start of the ice cover) the ice is typically fragmented, as aggressive seas infiltrate the ice canopy causing local floes to bend, fatigue, and fracture. In extreme seas the pummeling can create an outer band of ice slurry a few kilometers across, where it is difficult to distinguish individual floes, or an expanse of heavily deformed rafted sea ice. A little further into the ice pack, the seas will have lost some of their ferocity but they still control the FSD by breaking up substantial floes (Squire and Moore, 1980; Toyota et al., 2011). The MIZ is an interfacial region at the fringe of the open and frozen oceans, neither fully open nor fully frozen over — a mélange of ice cakes and floes, habitually pervaded by slurries of frazil ice and brash.

Ice floe sizes in the MIZ are generally smaller due to the wave-induced ice breakage, and ice cover is therefore normally less compact. Thus, internal stresses are less important than other forcing because the ice floes have more freedom to move laterally, and deformations occur more fluently compared to the plastic-like, discontinuous deformation of the compact

central ice pack. In this regime, internal stresses arise more from floe–floe contact forces than from any innate constitutive relation that embodies the behavior of sea ice at large scales. Thus, a model of the MIZ requires knowledge of how waves affect the FSD. Recognizing this, Shen et al. (1986) and Feltham (2005) have proposed granular-type rheologies for the MIZ that contain an explicit dependence on floe size, while others have presented direct numerical simulations of the MIZ using granular models with either a single floe diameter (e.g., Shen and Sankaran, 2004), or with floe diameters sampled from a power-law type FSD (Herman, 2013). Parameterizations for floe size dependent thermodynamical processes have also been developed (Steele et al., 1989).

Because the MIZ is the part of the ice cover closest to open sea, it is a very dynamic region that is significantly affected by changes to the incoming ocean waves and swells, and variations of winds and currents. Concentration is generally non-uniform, both spatially and temporally, and the disposition of the ice floes making up the zone is also normally quite heterogeneous as the waves break up floes differentially. Consequently, the observation that summer sea ice has become more MIZ-like throughout much of the Arctic Ocean is central to the processes we will study.

Additionally, wave–ice mechanics are central to a larger range of processes controlling the exchanges of momentum, heat, salinity, and moisture between the air–ice, air–ocean, and ice–ocean surfaces. Components of the DRI address each of these topics (Table 1). We will focus on the freeze-up period in the fall, when the open water fetch is at a maximum and the regional effects of sea state on the air–sea–ice system are expected to be most significant. This is also the period with the strongest storms, at least in recent years.

3 Science Objectives

- Develop a sea state climatology for the Arctic Ocean
- Improve wave forecasting in the presence of sea ice
- Improve theory of wave attenuation/scattering in the sea ice cover
- Apply wave–ice interactions directly in integrated arctic system models
- Understand heat and mass fluxes in the air–sea–ice system

These objectives are detailed in the following subsections.

3.1 In situ observations and climatology

In situ observations and climatology of the arctic sea state are needed to understand the role of waves in the emerging Arctic Ocean, both for practical applications (e.g., vessel operations)

Table 1: Processes, key variables, and related elements of the Sea State DRI.

Process	Key Variables	SeaState DRI Plan (by PI)
Wave reflection	Directionality	Wave buoy array (Doble/Wadhams), scattering models (Squire/Williams), viscoelastic models (Shen/Squire/Rogers), laboratory experiment (Shen/Ackley/Babanin/Squire)
Wave attenuation and dispersion	Ice distribution, ice thickness, wave spectra	Ship and AUV transects (Maksym/Ackley), wave buoy array (Doble/Wadhams), satellite observations (Lehner/Gemmrich/Holt), scattering models (Squire/Williams/Meylan/Bidlot), viscoelastic models (Shen/Squire), phase-averaged spectral models (Rogers/Babanin), laboratory experiments (Meylan/Shen/Ackley)
Wave generation	Ice cover, fetch, winds, boundary layer turbulence	SWIFT buoys and wave video (Thomson), Meteorological fluxes and LIDAR (Guest/Fairall), Marine Radar (Graber), Satellite observations (Lehner/Gemmrich/Holt), phase-averaged spectral models (Rogers/Babanin)
Ice formation	Ice distribution, heat loss, wave spectra	AUV and ship surveys (Ackley/Maksym), wave spectra (Doble/Wadhams)
Ice growth	Ice distribution, heat loss, wave spectra	AUV and ship surveys (Ackley/Maksym), UAV photography (Maksym/Doble), wave spectra (Doble/Wadhams), satellite observations (Lehner/Gemmrich/Holt)
Ice evolution	Transition to quiet growth, wave attenuation	AUV and ship surveys (Ackley/Maksym), wave spectra (Doble/Wadhams)
Heat and momentum flux	Radiative fluxes, turbulent fluxes, surface drag	Covariance observations (Guest/Fairall), AUV ice transects (Ackley/Maksym), SWIFT buoys (Thomson)
Heat storage	Temperature profiles, ice cover	Glider transects (Maksym/Stammerjohn), Acrobat and CTD (Stammerjohn), UpTempo buoys (Stammerjohn/Steele), Ice Mass Balance Buoys (Maksym)
Storm formation	Ice cover, clouds, winds	Meteorological observations and ceilometer (Guest/Fairall), SWIFT buoys (Thomson), satellite observations (Lehner/Gemmrich/Holt)
Wave climate	Wave height, period, direction	Satellite observations (Babanin, Lehner/Gemmrich), moorings (Thomson), phase-averaged spectral models (Rogers/Babanin)

and for science applications (e.g., improving model physics). Because no systematic studies of the wave climate in the Beaufort and Chukchi seas have been conducted, there is little information on the mean and extreme wave characteristics, such as wave height, period, direction, or the frequency of occurrence and duration of storms. All of these parameters are of great significance for oceanographic, meteorological, climate, naval, and maritime applications in the arctic seas. Apart from the North Atlantic region, however, this ocean until relatively recently has been frozen enough to prevent significant waves occurring. The past wave climate was non-existent; observations of the present climate are marginal and cannot be extrapolated into the future. To date, the longest reported time series of wave measurements in the Arctic Ocean is only a few years (Francis et al., 2011). A basic goal of the DRI is to increase observations of sea state conditions in the Arctic, specifically observations of winds and waves over a broad range of sea ice cover conditions. This will be accomplished with moorings, autonomous platforms, and ships, as detailed in the experimental plan (§ 4).

One approach to develop a sea state climatology in the absence of in situ data is to use model hindcasts or archived analyses such as the archives of the NOAA/NCEP (National Oceanographic and Atmospheric Administration/National Centers for Environmental Prediction) operational model, e.g., those from the operational WAVEWATCH III® model (herinafter WW3) from 1999 to the present. Figure 3 shows hindcast results for wave heights, along with measured winds and satellite-derived ice coverage near Barrow, Alaska. The fall period has higher winds and larger waves that coincide with minimum ice coverage. Before defining a climatology based on model hindcasts, however, the models must be validated. Ground truth data collected using moorings deployed throughout the DRI will be used to improve and evaluate wave models for the Arctic Ocean, such that a reliable climatology can be developed from the model output.

Other approaches to develop a climatology are to use remote sensing products, such as satellite altimeter data (Figure 4), or prediction and analysis of strongly-coupled future wave–wind–ice trends. These are motivated by both the short duration of the existing observations and the changing dynamic conditions for wave generation. Dobrynin et al. (2012), for example, show that climate change scenarios indicate a future increase of wind speed and wave height in the Arctic.

3.2 Wave forecasting in the presence of sea ice

Wave evolution, and thus the development of a sea state, is described by the radiative transfer equation or Boltzman equation, as follows:

$$\frac{\partial E}{\partial t} + \nabla \cdot (c_g E) = S_{\text{wind}} - S_{\text{brk}} + S_{\text{nl}} - S_{\text{ice}}, \tag{1}$$

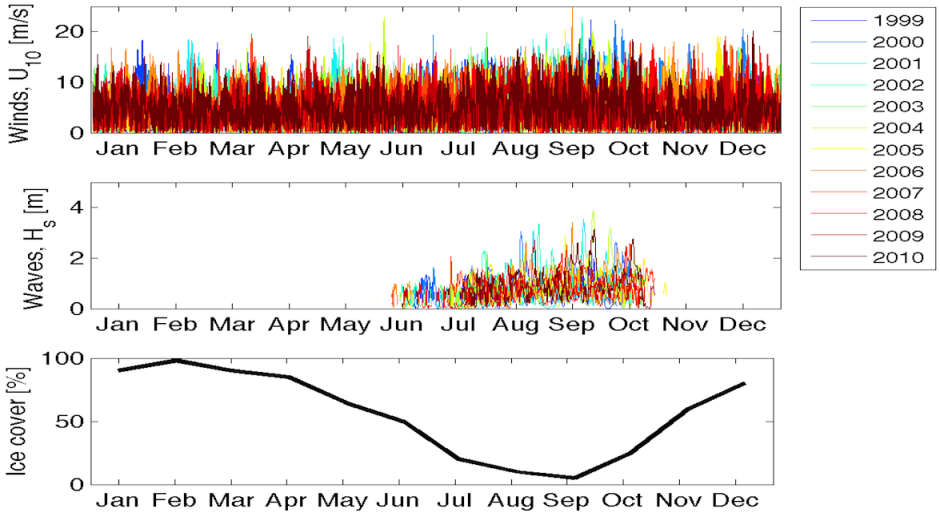

Figure 3: Measurements of wind speeds (top), model output of wave heights (middle), and satellite observations of average ice cover (bottom) near Barrow, Alaska. The increased wind speed and wave height during the open water season (Aug–Oct) coincide with increased storm energy. Image: J. Thomson and Y. Yu (unpublished).

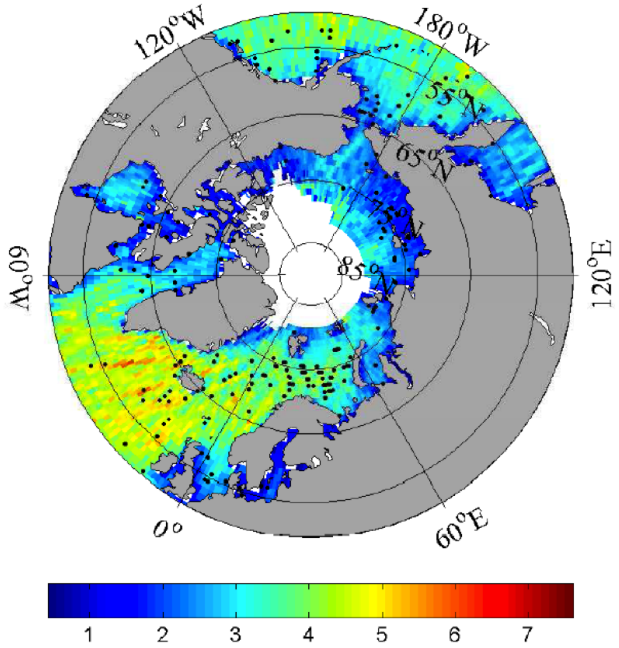

Figure 4: Satellite-altimeter-derived mean 99th percentile of significant wave height (m) in the Arctic region in September over 2002–2011 period. Image: A. Babanin (unpublished).

where E is the wave energy spectrum and c_g is the group velocity (Masson and LeBlond, 1989; Young, 1999). The equation describes the temporal and spatial evolution of waves as an energy budget. The deep-water source/sink terms are: input from the wind S_{wind}, dissipation via breaking S_{brk}, nonlinear interactions between wave frequencies S_{nl}, and interactions with sea ice S_{ice}. This is the basis of all contemporary, i.e., third-generation, wave prediction models such as the WAVEWATCH-III model from NOAA (Tolman, 1991, 2009) and the WAM model of the European Centre for Medium Range Weather Forecasting (ECMWF) (Bidlot , 2012). The first three source terms have been characterized in the open ocean but not in the presence of ice.

In open water, the wind input term, S_{wind}, can be estimated using the wind stress and a transfer velocity (Gemmrich et al., 1994; Terray et al., 1996; Donelan et al., 2006), although WW3 actually now uses calibrated theoretically based formulae to estimate the wind input term. In the presence of ice floes, the appropriate modification of this formulation is unknown. Previous observations suggest that wind–wave growth is reduced significantly in the presence of ice floes and that the resulting wave field has lower frequencies than that predicted for an open sea (Dozaki et al., 1999). In tandem, waves are preferentially attenuated by the sea ice, which also promotes the elimination of higher frequencies. We seek an accurate description of S_{wind} as a function of ice cover (as well as wind stress and transfer velocity).

The dissipation term, S_{brk}, can be estimated from in situ observations of turbulence in the water (Thomson, 2012; Gemmrich, 2010) and in the air (Iafrati et al., 2013), from statistics of the oceanside kinematics (Thomson et al., 2009; Gemmrich et al., 2008), or by directly combining probability of breaking occurrence and parameterizations of breaking severity [e.g., Filipot et al. (2010); see also Babanin (2011) for an overall review]. Recent observations report that turbulence dissipation is suppressed by ocean stratification (Vagle et al., 2012), suggesting that S_{brk} is sensitive to near-surface stratification and may be reduced during days with strong solar heat fluxes. The turbulent dissipation, in turn, is related to the turbulent surface heat fluxes. Thus, breaking dissipation in the Arctic may be quite different to that in the open ocean, because heat fluxes will be modulated by the presence of ice. We seek an accurate description of S_{brk} in the presence of sea ice and melt water.

The S_{ice} term itself is not included in the release versions of WAVEWATCH III or WAM. Rather, the default is to simply reduce wind input S_{wind} in the MIZ proportionally, depending on the known ice concentration. Several theories of wave–ice interaction exist in the literature, but two of them are well suited for use within a general framework; viscoelastic theory and scattering theory. The former treats the surface where ice is present as a continuous surface layer with physical properties different than those of the water. The latter considers the surface covered by a set of scattering elements of different sizes and different reflecting/scattering properties. While it seems reasonable to interpret the viscoelastic environment as representing

continuous solid ice and the scattering environment as broken ice characterized by a random distribution of separate ice floes, in fact the theories are compatible and related. When calibrated, the viscoelastic theory should be able to describe the floe-covered field in terms of its mean effect on the wavy surface, and the scattering theory is still applicable to heterogeneous quasi-continuous sea ice because of the presence of scattering from cracks, open and refrozen leads, and pressure ridges. Two simple formulations for S_{ice} were given by Masson and LeBlond (1989) and Meylan et al. (1997), which were subsequently shown to be identical (Meylan and Masson, 2006). The scattering term is much better modeled than the attenuation because the complete physics behind the wave attenuation is not known. Moreover, additional physics can be brought into the analysis and parameterizations, once a general theory is accommodated as the framework. Among these, two are highlighted: floe–floe collisions and ice–turbulence interactions. These mechanisms will add to the effects produced by the general mechanism. Both are dissipative, i.e., they will reduce the mean wave energy, and the former will also contribute to scattering the energy.

Although many formulations are now under development, a consistent approach to quantifying S_{ice} has not been identified. Detailed measurements of wave–ice interactions in a range of sea states are needed to assess the models now being developed. Recently, Doble and Bidlot (2013) implemented a non-conservative S_{ice} term in the ECMWF third-generation WAM model (WAMDI Group, 1988; Komen et al., 1984, 1994), designated 3GWAM subsequently, and have applied it to a hindcast of the Weddell Sea, and compared it with observations from a wave buoy. Rogers and Orzech (2013) also implemented two non-conservative S_{ice} routines in WW3, and applied and verified them using simple tests. Since then, a third S_{ice} formulation has been added using routines provided by H. Shen, a viscoelastic model. The WW3 code is maintained on the development repository at NCEP and is available to international co-developers. Continued development, and a comprehensive description of S_{ice}, is a principal objective of the Sea State DRI.

The main wave–ice interaction effects from the spectral modeling perspective are three: dissipation of wave energy (i.e., its loss from the wave field as opposed to attenuation in a particular direction of propagation); change of the wavenumber of wave components propagating into the ice fields; and scattering of the wave energy (which includes reflection from the ice edge). The first two effects can be accommodated in a new 'ice dissipation' term that should also pass information about wavenumber/group velocity to the advection term on the left-hand side of Eqn. 1 at each integration step. The third effect should be suitable to include in a separate conservative 'ice-scattering' term that changes the directional/frequency spectrum without dissipating the overall mean wave energy (see Section below). In the context of the viscoelastic parameterization of wave–ice interaction, such theory will produce an effective viscosity that will encapsulate the dissipation, and an effective modulus of elasticity

that will be used to estimate the change in wavenumber. Directional/frequency scattering can be parameterized by means of laboratory experiments, in principle, and two-dimensional surface modeling of waves in ice fields, before being verified in the field experiment. As the additional theories are incorporated, they may need to be parameterized in terms of additional energy source/sink terms, to allow us to use different formulations for different mechanisms and to have some mechanisms switched off (for example, floe–floe collision in solid ice) while others remain active.

Coupling is a critical component of any ocean wave forecast in icy seas because waves have the capacity to break up the ice floes that constitute the MIZ to create and repeatedly adjust the distribution of floe sizes, and to change local concentration (and hence wave fetch) by allowing floes to have more lateral freedom to move due to wind, waves, and currents. Moreover, the newly configured ice field then affects the passage of waves differently, with a multifaceted interplay occurring between the continuously evolving floe size and spatial distributions, and the resulting scattered (attenuated) wave field. From the coupled atmosphere–ocean perspective, the air–sea interaction regime evolves as the presence of waves and the open water alter the energy, momentum, heat, and mass exchanges, as well as surface roughness and sea drag. From the ice perspective, apart from possible breakage of the continuous pack ice and ice floes, the presence of waves affects ice formation and ice ablation or healing — depending on the local temperatures at the time. These processes define the ice-edge retreat and advance and, in turn, impact on the wave properties. In the longer term, waves and ice will be described by separate fully-coupled models. In the short term, for operational wave forecasting needs, a simple wave–ice coupling module can be accommodated within WW3 and 3GWAM to provide switching between the solid ice to partial coverage parameterizations and to define respective wave fetches.

Separate parameterizations should be sought for conditions of partial ice coverage and solid ice. The threshold needs to be set on what is regarded as solid ice in terms of ice coverage. At this stage, 90% coverage appears the reasonable threshold.

3.3 Wave attenuation and scattering by sea ice

The distance over which waves induce the sea ice to break, i.e., the width of the MIZ, is controlled by exponential attenuation of the waves imposed by the presence of sea ice. The rate of wave attenuation depends on wave period and the properties of the ice cover (Squire and Moore, 1980; Wadhams et al., 1988). Wave attenuation is modeled using multiple wave scattering theory or by models in which the ice cover is characterized as a viscous fluid or a viscoelastic material. In scattering models, wave energy is reduced with distance traveled into the ice-covered ocean by an accumulation of the partial reflections that occur when a wave encounters a floe edge (Bennetts and Squire, 2012a). Scattering models are hence strongly

dependent on the FSD. In viscous models (e.g., Weber, 1987; Keller, 1998) wave energy is lost to viscous dissipation, and presently no methods have been developed for these models to accommodate dependence on FSD. However, moduli in the viscoelastic model of Wang and Shen (2010, 2011) are expected to be greatly influenced by ice morphology, including the FSD. One of the goals in this DRI is to use an inverse method to determine the viscoelastic parameters for various types of ice covers. In reality, there is obviously a feedback between the FSD and wave attenuation, because the amount of ice breaking depends on how much incoming waves are attenuated and the amount of scattering depends on how much breaking there is — but the convenience of representing the whole sea ice cover as a continuum is undoubtedly compelling (although no evidence yet exists to show this simplification is valid).

Free surface ocean waves propagating into and traveling through pack ice can expect to encounter several different kinds of irregularity during their passage, particularly depending on physical location. Nevertheless, from a modeling perspective their progression will be determined by: (i) scattering from a distribution of sizes of discrete ice floes, present at some specified concentration, in the MIZ; and (ii) reflections from physical imperfections where the sea ice is less broken up and quasi-continuous, i.e., in the ice interior well away from any sizable areas of open water. In addition, energy will be lost from the advancing wave trains because of wave breaking, the natural inelasticity of the sea ice, and collisions between adjacent ice floes that are provoked by relentless wave action when the seas are rough. Each of these mechanisms causes some diminution of the wave amplitude in a manner that is known to favor the passage of long period waves over short periods. Consequently, the integrated effect of coming upon many heterogeneities over large distances is a gradual evolution of the wave spectrum towards longer period energy and the removal of short period waves, as explained in the reviews by Squire et al. (1995) and Squire (2007).

Previous measurements of attenuation, with the main contributions from Robin, Wadhams, and Squire (see again Squire et al., 1995; Squire, 2007), are relatively sparse because field experiments are logistically challenging and remote sensing instrumentation is only just reaching the necessary level of technological resolution. Modeling of the attenuation rates has received more attention (Squire et al., 1995; Squire, 2007), but earlier models are normally one-dimensional (1D, with the vertical dimension implicit) and it is only recently that the added complexity and numerical impediment of dealing with two-dimensional (2D) scattering theory could be contemplated. Notwithstanding, the passage of waves of different periods has been modeled across 1670 km of natural heterogeneous sea ice terrain in the Arctic extracted from submarine upward looking sonar profiles (Squire et al., 2009), demonstrating unequivocally how attenuation changes with wave period (Figure 5). More detail is provided in Figure 6 for a 22-s wave. Figures 5 and 6 represent an example of the best that can be achieved now with a 1D wave scattering model (see also Bennetts and Squire, 2012a,b),

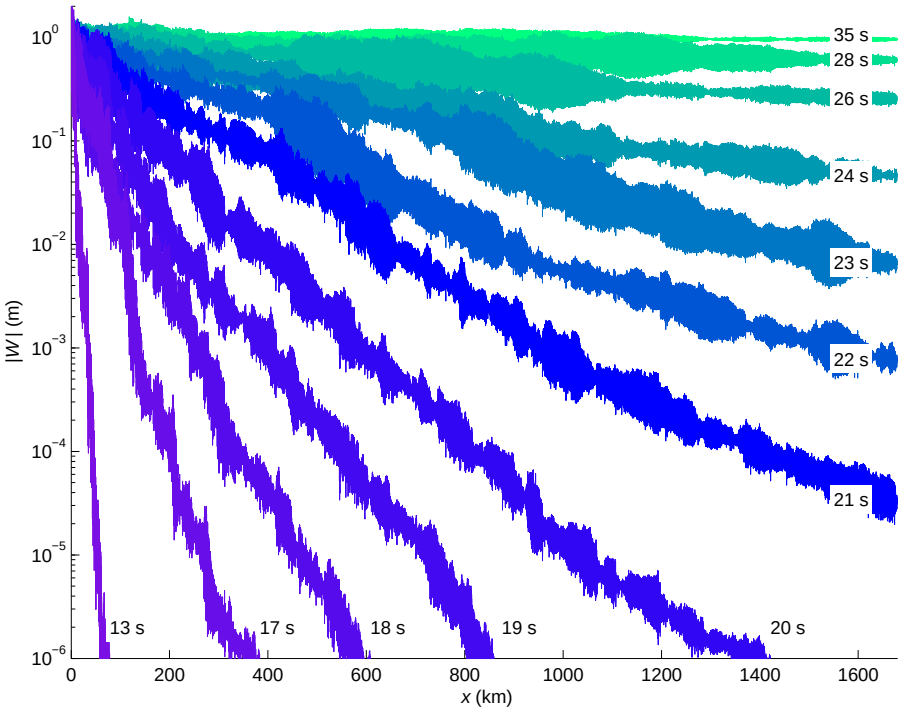

Figure 5: How the amplitude of ocean waves with period T ranging from 13 to 35 s is affected by 1670 km of ice terrain. Image: Squire et al. (2009).

i.e., any topography that may include pressure ridge sails and keels, any interfaces such as leads or cracks, and any choice of effective moduli within a recoverable elastic or viscoelastic paradigm — the latter being defensible because of the strain rates involved. Validation with actual measurements, and assessment of how this 1D treatment relates to the effects of the actual 3D ice topography with all its complexities, has yet to take place.

The continuum approach of Wang and Shen (2010, 2011) is similar in principle, but assumes that the ice–ocean system is modeled as a homogeneous viscoelastic fluid overlying an inviscid layer, both of finite thickness, which leads to additional wave modes. Its current drawback is that the sea ice field must be spatially uniform and that, to date, phase-resolving reflection and transmission coefficients at the water–ice interface or at changes of property have not been found precisely. Note, however, that this does not preclude abutting strips of sea ice, or 'cells', with different viscoelastic moduli together to follow how the wave energy moves from strip to strip, where resolution of the phase is less crucial and reflection at strip edges does not occur. The advance to modeling 2D scattering by ice floes and features in the sea ice and to eliminating homogeneity in the Wang and Shen model, potentially by accurately matching across strips in the manner of Squire (1993) to preserve phase, is a focus of the current DRI. Making the connection between the two approaches is also a goal, because the link to the scattering and dissipation that is really occurring can only be made

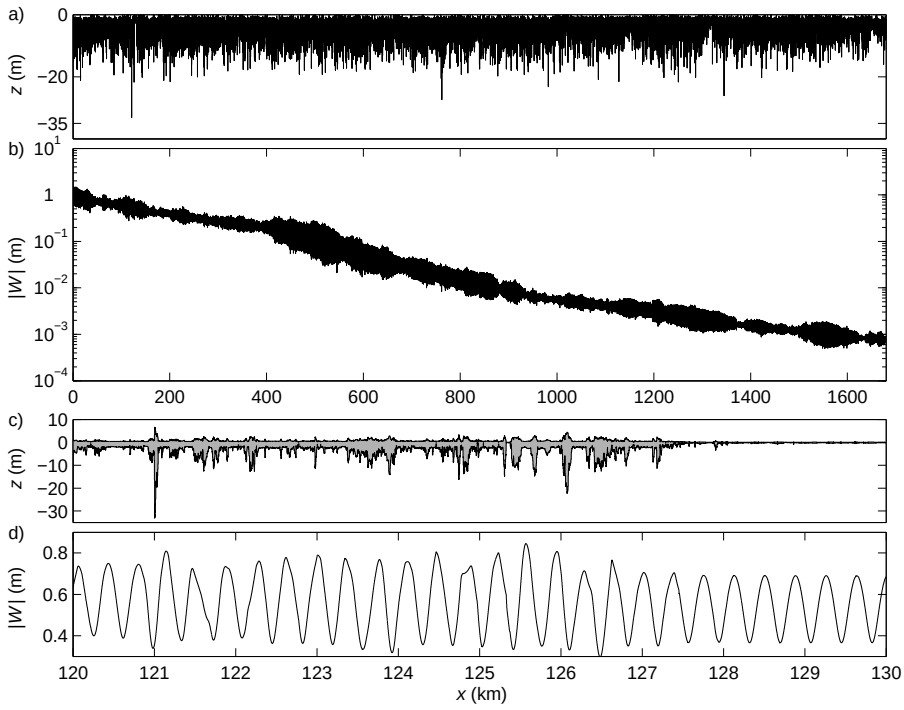

Figure 6: (a) The ice draft profile measured by submarine in 1994 and archived data NSIDC; (b) vertical displacement $|W|$ of a 22-s wave as it progresses through the entire 1670-km transect; (c) a 10-km example of the thickness profile used in the model, showing ridge sails and keels; and (d) 10-km detail of the modeled vertical displacement $|W|$. Each is plotted against the horizontal coordinate x. Image: Squire et al. (2009).

by calibration. Such an approach also takes us away from focusing understanding on the real processes involved, replacing the sought-after actual physical parameterizations with computationally tractable phenomenological ones. It has, however, been largely successful at producing other terms for wave modeling, such as dissipation by wave breaking S_{brk}, for which the physics also are not well understood.

Wave scattering by a single floe and by either a modest number of floes or by many floes with an imposed artificial periodicity condition, has been modeled successfully by several researchers (e.g., Peter & Meylan, 2009; Bennetts and Squire, 2009). Because of the averaging effect of many ice floes, the disk is regarded as a prototype shape to synthesize 2D ocean wave scattering in the MIZ, noting that more complicated forms are also possible if required (see Peter & Meylan, 2009; Bennetts and Williams, 2010). Unfortunately, although mathematically tractable, the computation is numerically prohibitive even for simple disks because the scattered waves from every disk present interact with every other disk. We are developing and will continue to develop efficient iterative procedures that allow us to specify the level of multiple scattering sought and a radius of action that dictates a maximum

distance over which floes interact, this being a physically plausible model for a MIZ as it assimilates a parameterization for the supplementary nonlinear effects. Moreover, we will be developing a method to decompose the circular wave fronts generated by ice floes in motion into an angular distribution of plane waves, a necessary step to solving what happens when a directional open sea wave spectrum impacts on an ice field.

The primary shortcoming of all models developed so far is that they either assume that the energy is conserved or they impose an arbitrary dissipation based on a non-measurable parameter. The most significant unanswered question is to determine the process or processes by which energy is dissipated as it propagates through a field of broken ice.

There is a dearth of data in regard to the directional evolution of ocean waves entering an ice field. Indeed, the only field study (Wadhams et al., 1986) is now over 25 years old and reports results that are thought provoking but not comprehensive [see also Liu et al. (1991b)]. Contrary to what was conjectured at the time, recent modeling efforts are suggesting that the effect of an ice field is to broaden the directional spread of an entering wave spectrum to a degree that depends on penetration distance and frequency. In fact, angular spread within the ice cover apparently soon becomes entirely isotropic. With hindsight, this is not unreasonable, as we now know that in the MIZ scattering is the dominant influence over path-dependent attenuation (Wadhams et al., 1986). It is vital that we understand this process, because it is the wave scattering from the ice floes that make up the MIZ, along with modification of the FSD by wave-induced breakage, that will feed directly into modeling progress as we make the anticipated step from 1D to 2D models. Field measurements are clearly required to resolve the change in directionality with penetration and validate or refute the modeled hypotheses.

A theoretical model to replicate the results of Wadhams et al. (1986) is not straightforward but appears to be possible. Moreover, the theory could transition directly into a WIFAR[3] type ice–ocean model if constructed appropriately. The issue is that every floe in the MIZ acts like a point source for waves when it is brought into motion by the incoming long-crested sea and swell (i.e., it creates circular wavefronts that propagate radially and interact with adjacent and more distant floes in its vicinity). The challenge is not with the interactions, which can be modeled precisely mathematically subject to computing power (observing that the quantum of multiple scatterings and radii of action can be optimized), but with converting these circular wave fronts into a spectrum of long-crested ocean waves as these waves advance further into the ice field. This is what is required to track the steady progression of incident seas and swell farther and farther into the MIZ, to provide both the attenuation and changes to directional spread. In its simplest form this is about expressing radial waves as a sum

[3]Waves-in-Ice Forecasting for Arctic Operators, a NERSC-led project. See `http://www.nersc.no/project/wifar`

of plane waves traveling in the positive (for $x \geq 0$) and negative ($x \leq 0$) directions, which mathematically is

$$\mathrm{H}_n(kr)\mathrm{e}^{\mathrm{i}n\theta} = \begin{cases} \dfrac{(-\mathrm{i})^n}{\pi} \displaystyle\int_{-\pi/2+\mathrm{i}\infty}^{\pi/2-\mathrm{i}\infty} e^{\mathrm{i}n\alpha} e^{\mathrm{i}k(x\cos\alpha + y\sin\alpha)}\,\mathrm{d}\alpha, & x \geq 0, \\ \dfrac{\mathrm{i}^n}{\pi} \displaystyle\int_{-\pi/2+\mathrm{i}\infty}^{\pi/2-\mathrm{i}\infty} e^{-\mathrm{i}n\alpha} e^{\mathrm{i}k(-x\cos\alpha + y\sin\alpha)}\,\mathrm{d}\alpha, & x \leq 0. \end{cases} \tag{2}$$

Once we can compute the plane wave spectrum that is reflected from the ice edge and the one that is transmitted through a rectangular strip of MIZ parallel to the edge, the effect of the MIZ as a whole in attenuating and spreading the waves radially can be found by patching together many strips and using transfer matrices.

The above analysis provides a theoretical pathway to link the scattering theory and the viscoelastic continuum model. Because scattering reduces the forward going wave energy, it acts as an effective attenuation. Via an inverse method, it is possible to use the data from the scattering theory to determine the viscous parameter in the viscoelastic theory.

An alternative approach to understanding the directional spread of wave energy is to use the radiative transfer equation (1), as used by Meylan et al. (1997). Under conservative wave scattering the wave field was shown to rapidly become isotropic and this rate was shown to be frequency dependent.

3.4 Arctic system models with wave–ice interactions

An overriding goal driving the theoretical advances has been to properly embed interactions between ocean waves and sea ice into ice–ocean models and, potentially, ocean general circulation models (OGCMs) — the surface wave field being an attribute of sea ice dynamics that is currently conspicuous by its absence in contemporary ice–ocean models. Yet, the notion and importance of integrating wave–ice interactions into an ice–ocean model is not new; indeed it was broached more than two decades ago. Since then, several authors have presented numerical models for transporting wave energy into ice-covered fluids. Masson and LeBlond (1989) were the first to incorporate the effects of ice into the wave energy transport/balance equation that had previously been used to model waves in open water only (Gelci et al., 1957; Hasselmann, 1960; WAMDI Group, 1988; Ardhuin et al., 2010). Masson and LeBlond (1989) studied the evolution of the wave spectrum with time and distance into the ice and their theory was used subsequently by Perrie and Hu (1996) to compare the attenuation occurring in the ice field with experimental data. Meylan and Masson (2006) and Meylan et al. (1997) derived a similar transport equation to that of Masson and LeBlond (1989) using the work of Howells (1960), and concentrated on the evolution of the directional spectrum. Although they neglected nonlinearity and the effects of wind and dissipation due

to wave breaking (see Eqn. 1), they improved the floe model by representing the ice as a compliant plate rather than as a rigid body. Doble and Bidlot (2013) also recently extended the ECMWF WAM into the ice in the Weddell Sea, Antarctica, using the attenuation model of Kohout and Meylan (2008). While this model does not allow for directional scattering, it does include the usual open water sources of wave generation and dissipation by the same method as Masson and LeBlond (1989) and Perrie and Hu (1996). Modeling capabilities have now reached a level of sophistication at which a numerical description of wave evolution through an ice pack that resembles the natural phenomenon is possible. As noted, work in this area has largely been 1D (Kohout and Meylan, 2008; Vaughan et al., 2009; Squire et al., 2009); 2D extensions are also being developed (Bennetts et al., 2010) but are so far subject to unrealistic simplifying conditions for a real MIZ.

Mathematical models are primarily intended to explain how ocean wave trains evolve spatially as they proceed through fields of sea ice. However, in an ice–ocean model these results have a direct bearing on sea ice morphology too because the capacity to damage floes will depend on the local wave energy (Vaughan and Squire, 2011). This interdependence is the basis of a 1D ice–ocean model (Dumont et al., 2011a) that is now being extended to an operational 2D model (i.e., the ocean surface, and is seen as a precursor to full assimilation into an arctic system model). Conceding that their ice breaking criterion is not yet perfect, Dumont et al. (2011a) are the first to include ice breakage in a wave transport problem. Previous studies modeling ice fracture (e.g., Langhorne et al., 2001; Vaughan and Squire, 2011), only looked at general properties of the ice cover such as the lifetimes of ice sheets and the width of the MIZ. The method they used involved modeling the attenuation of an incident wave spectrum and defining probabilistic breaking criteria to decide when the strains in the ice would exceed a breaking strain. Dumont et al. (2011a), on the other hand, provide a fuller description of the resulting ice cover, estimating the spatial variation of floe sizes throughout the entire region where breaking occurs and also allowing the temporal evolution to be investigated. In addition, their model considers the coupling between the breaking and the transport of wave energy. Following this work, the archetypal Fram Strait MIZ was modeled in the WIFAR project being coordinated from NERSC (Dumont et al., 2011b; Squire et al., 2013; Williams et al., 2013a,b), as a first full step to absorbing wave interactions into an ice–ocean model; in this case TOPAZ [(Towards) an Operational Prediction system for the North Atlantic European coastal Zones], a hybrid coordinate ocean model of roughly 13-km horizontal resolution forced by ECMWF atmospheric fields (see Figure 7). The enhancement of WIFAR and its reconfiguration to the arctic system is a supported project within the DRI. Although these models are now 1D, i.e., they only consider a transect of the ocean, they are theoretically generalizable to include the second horizontal dimension.

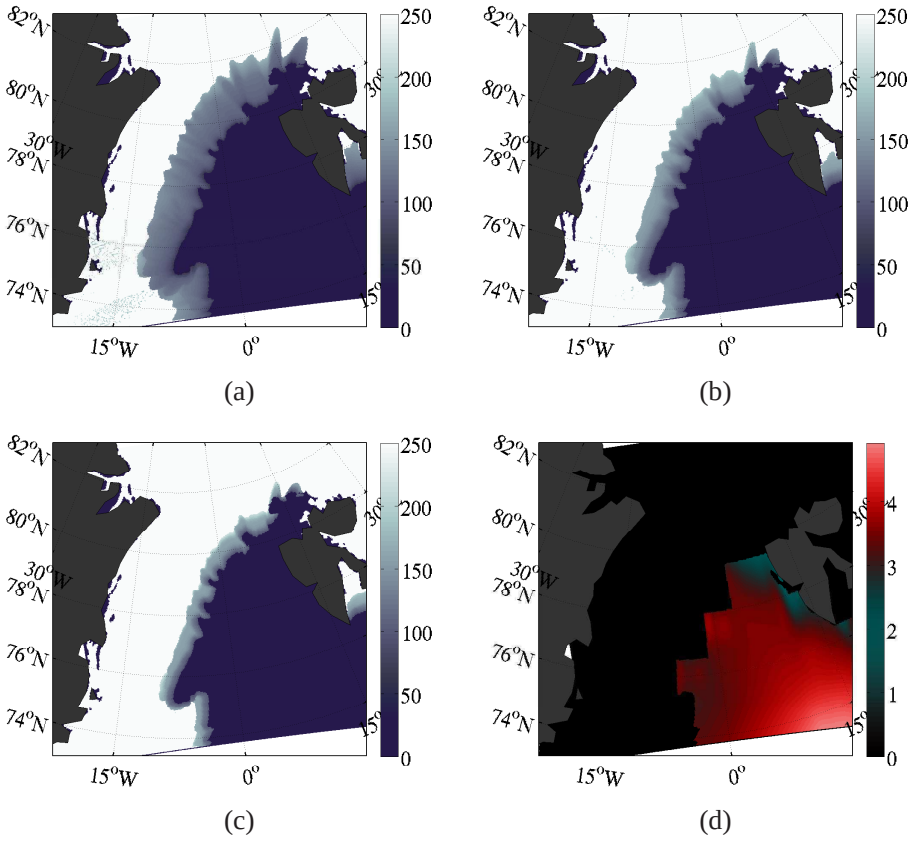

Figure 7: Maximum floe size in meters for different thicknesses (a–c), significant wave height H_s (d) (after WIFAR). Ice concentration is 0.8. Ice thickness is (a) 2 m, (b) 3 m, and (c) 4 m. Mean peak period is 10.5 s, mean wave direction is $187°$ with ten wave directions between $-9°$ and $221°$ included at a resolution of $21.2°$. Image: T. Williams (unpublished).

3.5 Heat, mass, and momentum fluxes

The fastest sea ice changes in the Arctic are happening during the transitional seasons. For example, over 1979 to 2010, the sea ice retreat occurred 48 days earlier and the sea ice advance occurred 42 days later in the greater Chukchi Sea region. A late autumn sea ice advance now often follows an early sea ice retreat. These seasonal sea ice trends are consistent with the expected seasonal feedbacks, e.g., an earlier spring breakup leads to increased solar ocean warming and accelerated sea ice retreat, while the additional solar heat gained by the ocean must be removed before sea ice can grow, slowing autumn sea ice advance. Further, an overall thinner, more seasonal arctic sea ice cover (as observed) enhances the feedback: less latent energy is required to melt a thinner sea ice cover, thus making available more sensible energy to warm the ocean. Finally, the lengthening of the summer open water season also means a longer period of wind–wave forcing on the upper ocean, together with changes in upper ocean heat and freshwater content. Together, these changes affect subsequent freeze

onset and sea ice formation processes.

Another Sea State DRI objective is to examine the change in ice–ocean–atmosphere fluxes under a now stronger influence of ocean waves (Francis et al., 2011) before and during autumn sea ice formation. We hypothesize that stronger air–sea interaction in the fall period now exists, because of ice-free conditions, as evidenced by increased ocean heating (Perovich et al., 2007) and warmer air temperatures (Screen and Simmonds, 2010a,b) in late summer. The impacts of this interaction can include: observed increases in storminess and precipitation in summer–fall (Screen et al., 2011; Simmonds and Keay, 2009); presumed increased turbulence in the water column; observed delays in ice growth and (presumed) thinner sea ice because of higher ocean heat content (Stammerjohn et al., 2011, 2012); and presumed changes in modes of ice formation (frazil and pancake ice) because of waves (Lange et al., 1989; Shen et al., 2001; Ackley et al., 2002). Given the new summer sea ice regime in the Arctic Ocean without remnant multiyear ice and the trend towards delayed autumn sea ice advance, several different scenarios of seasonal ice formation and ice thickness evolution might occur. Direct measurement of heat and mass fluxes under these new conditions is therefore crucial to predict the future course of the arctic sea ice cover with confidence.

Historically, weather forecast models have diagnosed surface turbulent fluxes (including the stress) through bulk meteorological formulae

$$\langle w'x' \rangle = C_x U (X_s - X_r), \tag{3}$$

where w' is the turbulent vertical velocity fluctuation, x' is the fluctuation of the meteorological variable (horizontal wind speed, temperature, humidity), C_x is the transfer coefficient for X, U is wind speed, X_s the mean value of X at the surface, and X_r the mean value of X at some reference height z_r. The transfer coefficients have dependencies on surface stability and the surface properties. For example, the atmospheric momentum flux (i.e., wind stress) is

$$\tau = \langle w'u' \rangle = \rho_a C_D U_{10}^2, \tag{4}$$

where ρ_a is the density of air and $C_x = C_D$ is simply the drag coefficient. The actual turbulent fluxes (i.e., Reynolds stresses in the case of momentum flux) are best determined by direct covariance estimates, but the transfer coefficients and bulk fluxes are much more practical for use in models. Direct flux measurements will be a focus of the Sea State DRI field campaign, from which we seek to determine robust estimates of transfer coefficients as a function of sea state and sea ice.

For example, the atmospheric drag coefficient is known to depend on the surface roughness of ice (Andreas et al., 2010a,b) and waves (Young, 1999). However, many factors can affect wind stress in variable ice cover surfaces and adjacent open ocean regions (Guest et al., 1995) such that roughness alone does not predict drag (see Figure 8). More stable surface air

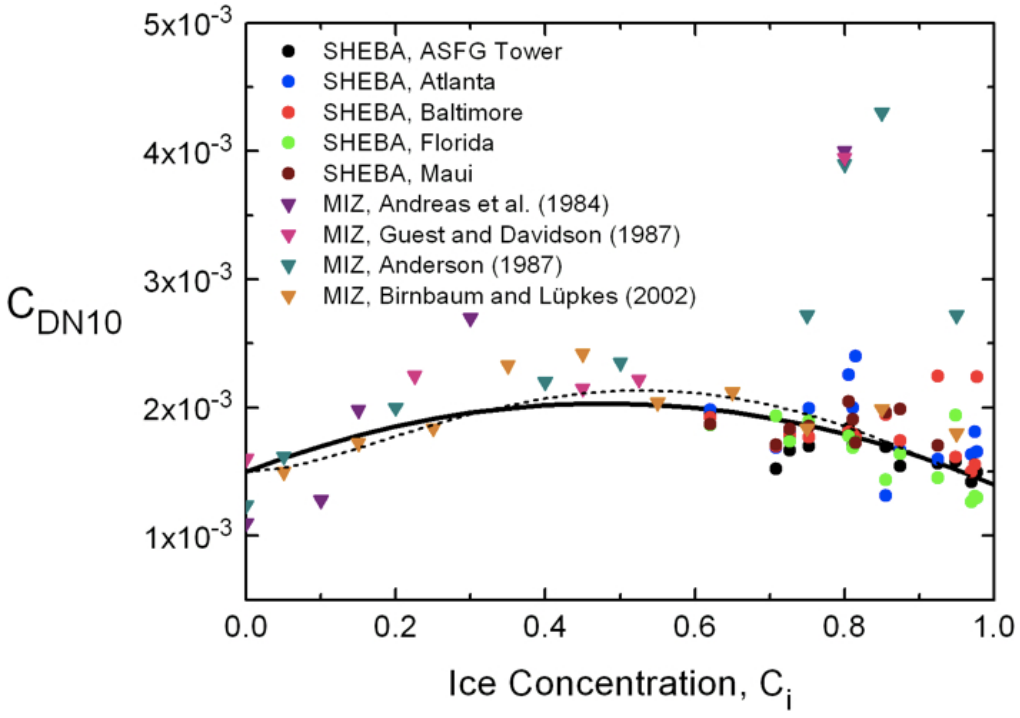

Figure 8: Atmospheric drag coefficient as a function of ice cover. Image: Andreas et al. (2010a).

masses over areas with more sea ice slow the surface wind. Baroclinicity in the atmospheric boundary layer over variable ice coverage regions and coastal areas caused by variations in surface fluxes creates wind shear and 'ice breezes' that may occur on scales smaller than forecast model grid sizes. The resulting curl in wind stress that often exists in these regions can generate vertical motions in the ocean (Guest and Davidson 1991b). Radiosonde and aircraft measurements from the MIZEX/CEAREX experiments revealed significant average variations in atmospheric boundary layer height and thermal structure, wind speed, surface turbulent and radiative heat fluxes, and cloud conditions across the MIZ (Guest et al. 1995) and sometimes the generation of fronts and mesoscale cyclones (Rasmussen et al. 1997). Determining surface fluxes in regions such as the Beaufort and Chukchi seas with highly variable surface conditions is difficult because the standard surface layer assumption of horizontal homogeneity is not valid.

The most striking gradients are in the albedo. However, ice regions and adjacent open ocean areas are also regions with strong horizontal contrasts in surface moisture, temperature, surface roughness, and wind vector (Guest et al. 1995). These contrasts create significant advection and associated turbulent surface fluxes that must be considered along with solar

and longwave radiation effects. Cloud conditions also often vary across these regions; these have important implications for changes in the net radiation budgets at the surface and associated feedback effects involving sea ice. We seek coordinated measurements of temporal and spatial variability of these fluxes, coincident with measurements of upper ocean properties, ice evolution, and sea state.

Beyond the bulk flux approach (Eqn. 3), coupling systems in the modeling community are moving toward a more holistic approach, in which a momentum budget is considered, and so it becomes increasingly important to have datasets with greater detail in this regard. In the context of the atmosphere, it is useful to know not just the wind stress, but rather to partition the stress: what fraction of momentum flux goes to the oceanic mean flow, the waves, and the ice? In the context of the ice cover, we seek improved quantification of the fraction of momentum delivered by the mean flow, the atmosphere, and the waves in turn. A specific key process that is poorly understood is the pressure momentum transport over waves. The total momentum flux can be partitioned into viscous, turbulent, and wave-correlated (pressure-induced) components, and the field campaign will target direct observations of these individual components. Improved understanding of small scale process such as this will build towards the larger context of comprehensive flux prescriptions in coupled models.

4 Work Plan

4.1 Remote sensing

Remote sensing, particularly satellite SAR (synthetic aperture radar) and altimeter data (Table 2 and Figure 9), will be used to quantify waves and ice over large spatial and temporal scales. These data will be essential to provide context and operational guidance for in situ measurements, as well as for developing climatology. Satellite acquisitions will be prioritized by the science team during Sea State DRI meetings and used to plan the 2015 cruise track.

Spaceborne radar altimeters have observed the oceans for more than two decades with an almost continuous record since 1985. Pulse-limited radar altimeters can estimate wave height about every second over a footprint of 1–10 km while the precise size depends on various characteristics (i.e., range, pulse width, and wave height). Satellite altimetry is also able to provide information on surface winds and on storm events, and on the respective trends in these quantities. Satellites equipped with altimeters operate on various orbits, which determine the repeat cycle, inclination angle, altitude, etc. With a change in the inclination angle, global coverage and repeat cycle also change. An inclination angle close to 90° yields better data coverage in the polar regions. In this regard, coverage of instruments operated by NASA/CNES (i.e., JASON1/2, TOPEX) ends at approximately 67°N/S. Altimeters of the

European Space Agency cover up to 80°N/S and higher. Beginning with the ERS1 launch in 1991, satellite coverage extends up to 82°N, with the latest Cryosat2 altimeter measuring waves and winds up to 88°N (provided these waters are open). Therefore, information on wave climate is available during much of the modern arctic MIZ era. For example, Figure 4 shows the mean of the 99th percentile significant wave height for the arctic in September, over the period 2002–2011.

Higher resolution wave and wind information can be retrieved from space-borne SAR sensors. Here we will use data from the X-band high-resolution SAR satellite TerraSAR-X (TS-X), which was launched in June 2007, and its twin TanDEM-X (TD-X), launched in June 2010. TS-X and TD-X operate from 514-km height at sun-synchronous orbits, with ground speed of $7\,\mathrm{km\,s^{-1}}$ (15 orbits per day). Both satellites are orbiting in a close formation with typical distances between satellites of 250 m to 500 m. They operate with a wavelength of 31 mm. The repeat-cycle is 11 days, but the same region can be imaged with different incidence angles after three days, dependent on scene latitude. Typical incidence angles range between 20° and 55°. The coverage and resolution depends on satellite mode: *ScanSAR* mode covers a 100-km strip, *StripMap* mode covers 30 km by 50 km with a resolution of about 3 m, *Spotlight* covers 10 km by 10 km with resolution of about 1 m. A new option, particularly useful for ice coverage investigation is the *Wide ScanSAR* mode, which covers 450 km by 250 km with resolution of about 40 m.

SAR is capable of providing wind information over the ocean by measuring the roughness of the sea surface. Retrieval of wind parameters from TS-X data is based on the XMOD-2 algorithm, which takes the full nonlinear physical model function into account. At the same time the corresponding sea state can be estimated from the same image. The empirical model for obtaining integrated wave parameters is based on the analysis of image spectra, and uses parameters fitted with collocated buoy data and information on spectral peak direction and incidence angle. The newly developed XWAVE-2 algorithm derives significant wave height, wave direction and wave length directly from TS-X SAR image spectra without using a priori information.

To describe the sea ice conditions, multiple types of remote sensing fine resolution imagery will be utilized. The key ice observations include FSD, ice type, open water and ice concentration, and ice morphology, with each observation useful for examining the impact of waves on the ice cover. Fine resolution imagery, as provided by SAR and optical sensors, is required to properly observe wave–ice conditions. For example, Toyota et al. (2011) identified a regime shift for floes less than 40 m in diameter and a resulting change in floe size distribution using high-resolution imagery. In addition to TerraSAR-X, SAR imagery from Sentinel-1 (scheduled for launch in late 2013) will also be utilized. The primary Sentinel-1 SAR mode has a swath width of 250 km and resolution of 5–20 m. Optical and thermal IR data of value

will be requested from ASTER and Landsat-8 (each sensor has resolutions of 15 m for the optical bands and 90 m for the thermal IR bands). Declassified very fine (1 m) resolution optical imagery will also be requested. Both high-resolution SAR and optical sensor imagery have been shown to provide useful and unique measurements of the listed ice parameters. Multiple fine resolution sensors are required to ensure optimal spatial and temporal coverage and to account for varying cloud and weather conditions, which may reduce the usefulness of the imagery. Larger scale observations of the ice edge, ice concentration, and the onset of ice melt and freeze-up, will use coarser resolution data and derived products generated by MODIS, passive microwave, and scatterometer data. Currently no remote sensors will be used to obtain either direct or freeboard-derived sea ice thickness measurements, a measurement made even more difficult within the MIZ and during fall conditions.

In preparation for the field experiment in 2015, wind, wave, and ice parameters will be monitored via TS-X and other data in September–October for both 2013 and 2014. Throughout the field campaign the remote sensing will be coordinated with the in situ observations, as well as the various long-term mooring sites.

In addition to the satellite remote sensing, in-field remote sensing will be employed, using small unmanned aerial vehicles (UAV), balloons, and manned aircraft (funded by other programs, e.g., IceBridge). Also, a shipboard marine radar and LIDAR systems will be used to measure ice cover and waves. The marine radar is particularly well-suited to measuring the directional distribution of waves, although recent work has also shown promise in estimating wave height. Shipboard LIDAR systems can measure the roughness and heights of both ice and water at fine scales, although the ranges are limited relative to the radar systems.

Table 2: Satellite remote sensing data (by PI), products, and scales.

Data	Products	Scales
SAR (Lehner/Gemmrich, Holt)	Wave direction and wavelength, wave propagation, ice cover and floe size distribution	1 m - 100 km
Altimeter (Babanin)	Wave height	1 km - 10 km
ASTER and declassified high-resolution imagery (Holt)	Ice cover and floe size distribution	10 m - 1 km

4.2 In situ observations

4.2.1 *Sikuliaq* cruise (fall 2015)

The primary observational component of the Sea State DRI will be a research cruise in the fall of 2015. A UNOLS ship time request (STR # 103422) has been submitted for the R/V

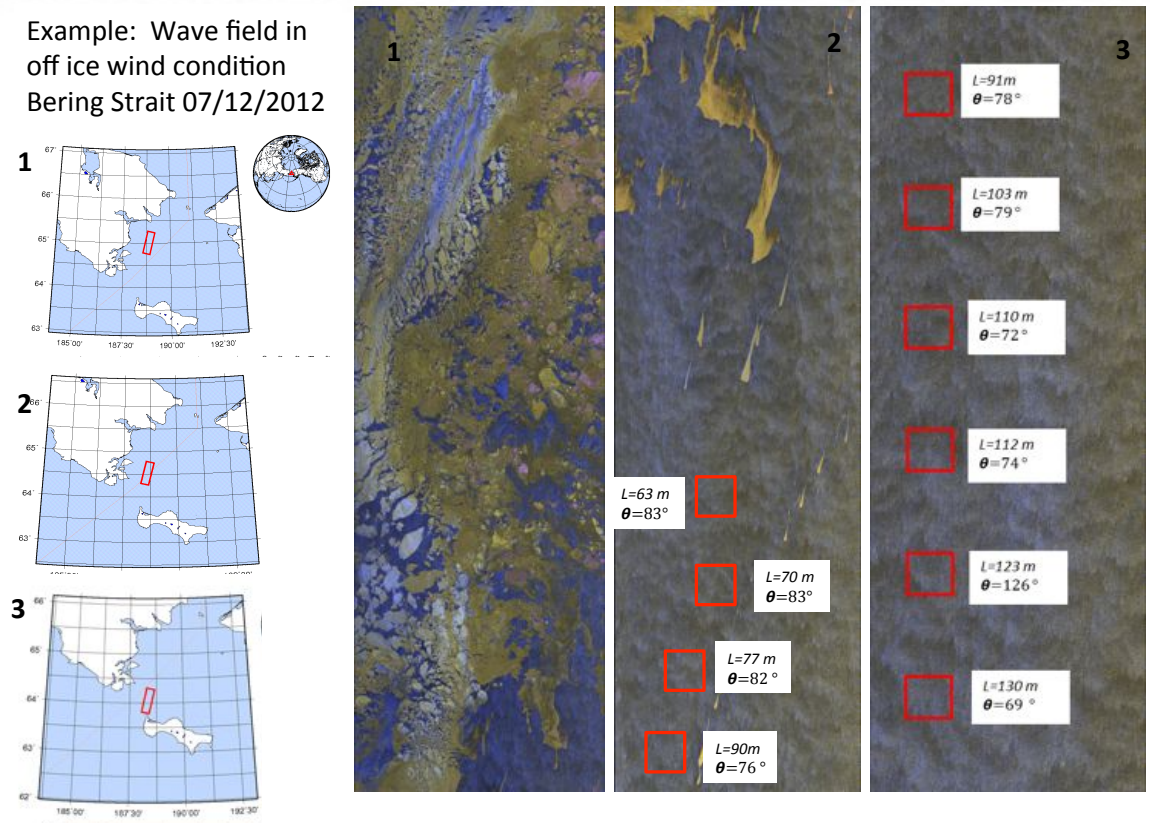

Figure 9: Example of wave and ice measurements from TerraSAR-x satellite observations. Image: T. Lehner and J. Gemmrich (unpublished).

Sikuliaq. The requested departure date is 20 September 2015 from Nome, Alaska, for a duration of 38 days. The cruise will be organized in a series of modules, each targeting specific processes from the science objectives and each emphasizing a subset of observational assets. Both shipboard (e.g., CTD casts) and autonomous measurements (e.g., wave buoys) will be employed during the cruise, often simultaneously. Mooring observations will supplement the cruise with long time series measurements. Table 3 lists the observational assets and Table 4 provides additional details on the buoys. Figure 10 shows the field observations schematically. Additional assets, such as unmanned aerial vehicles (UAVs) for photographic mapping of FSD and wave breaking crest distributions, are under consideration and will likely be included. A remotely operated vehicle (ROV) may also be included.

The notional R/V *Sikuilaq* cruise track and sampling locations are shown in Figure 11. The actual cruise track will depend on the ice and weather conditions during the cruise, and will be guided by forecast models and remote sensing products. The 2013 and 2014 seasons will be used as test scenarios, which the science team will use to determine optimal sampling for hypothetical cruises during those years. Sampling modules will be selected and tuned as conditions develop along the cruise track, such that transit days are minimized. Some assets,

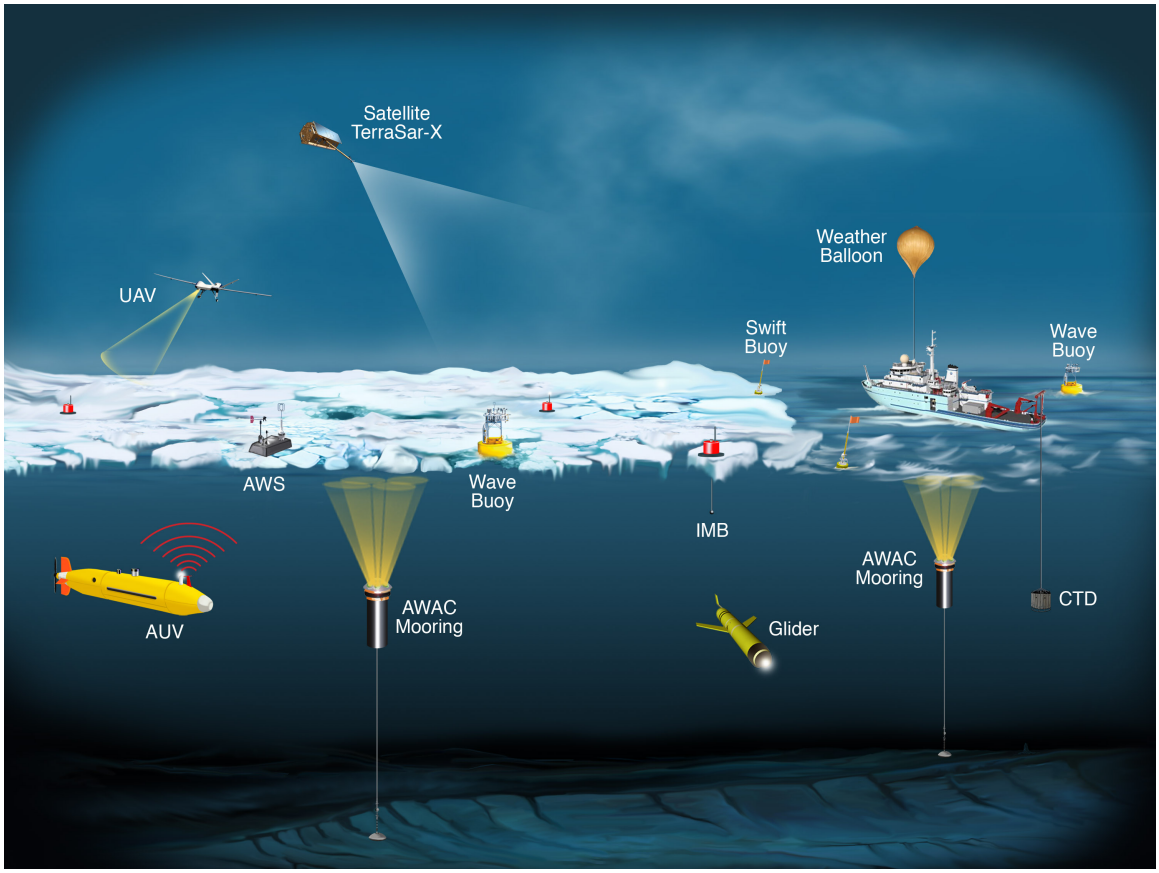

Figure 10: Schematic of measurement platforms for the Sea State DRI. Image: Woods Hole Oceanographic Institution.

such as gliders, may be operated continuously across different modules. Total transit days are estimated as approximately 14 days, leaving approximately 24 days for science activities. The sampling modules and nominal allocations are:

- **Open Water (6 days):** As part of the transit to reach the late summer ice edge, open water measurements of waves, winds, surface fluxes, and upper ocean profiles will be made from the R/V *Sikuliaq*. Shipboard measurements will be made both underway and holding station. During stations, autonomous buoys will be deployed for short drift missions (several hours) coincident with glider missions. Sampling will target a range of wave and wind conditions, with priority for sampling at least one storm, if and when the opportunity arises. The goal of this module is to quantify the evolution of a sea state in the presence of a variable fetch (which is unique amongst the world's oceans) and the subsequent effect on the heat and momentum in the upper Arctic Ocean.

- **Solid Ice Edge (6 days):** Upon reaching the late summer ice edge, a wave reflection study will be conducted using an array of wave buoys deployed along the ice edge and

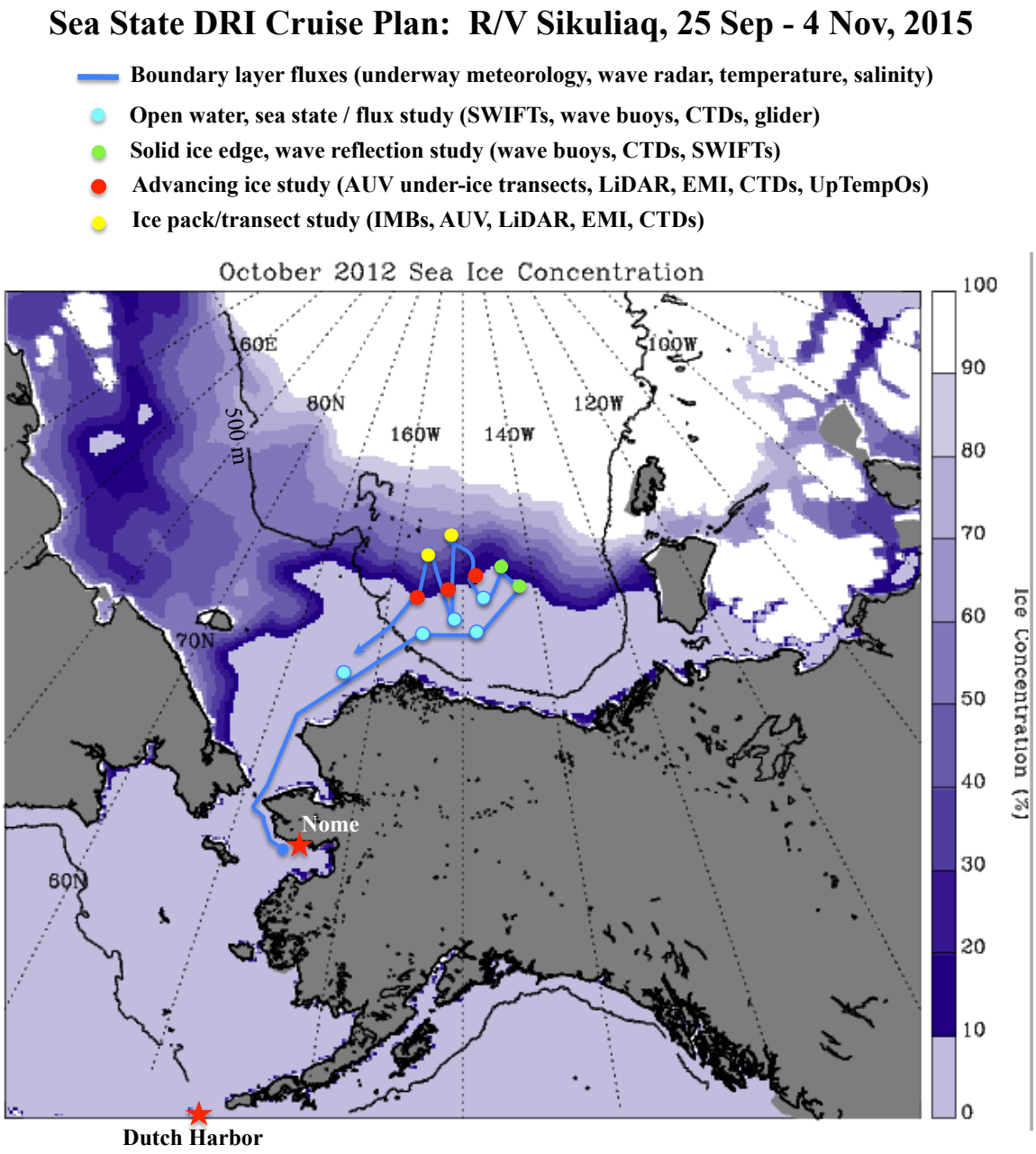

Figure 11: Proposed cruise track and sampling modules for the R/V *Sikuliaq*.

up to several kilometers into the ice pack. An AUV will be used to survey under the ice along the array, measuring ice thickness distribution (ITD) and FSD, as well as upper ocean properties. The R/V *Sikuliaq* will be used to tend the buoys and maintain the array while also surveying the ice. Ancillary measurements of meteorological forcing (winds and fluxes) and ocean response (CTD casts, ADCP transects) will be made as time permits. The goal of this module is to quantify the reflection of waves from a solid ice pack, in particular their directional distribution upon reflection and their spread upon farther penetration into the sea ice.

- **Advancing Ice Edge (6 days):** As cooling occurs and ice formation begins, measurements will focus on the advancing ice edge. This module will be further sub-divided into spatial series (transects) and time series (station keeping). The spatial series will combine ship and AUV transects of the ice, along with wave attenuation measurements by buoys. The time series will measure waves, ice growth and characteristics, ocean heat changes, ocean drag profiles, and boundary layer meteorology as a station evolves from open water to ice-covered. The goal of this module is to see how ice growth and edge advance affect ocean heat storage, sea state evolution, and atmospheric coupling.

- **Ice Pack (6 days):** Transects and stations into the ice pack, within the limitations of the *Sikuliaq*, will characterize the newly formed ice via coring, IMB deployments, LIDAR + AUV mapping, current profiling (for drag estimation), and meteorological measurements. The goal of this module is to understand the transfer of heat and momentum between air, sea, and ice as new ice forms, and to contrast these processes with the wave driven processes that occur in open water. We will also continue to examine the connection between incident wave conditions and the evolution of the ice pack (FSD, ITD, etc).

4.2.2 Moorings (2012–2015)

In addition to the intensive sampling during the cruise in 2015, mooring observations will provide long time series for context and evaluation of model climatology. Annual deployments of Acoustic Wave and Current (AWAC) instruments on sub-surface moorings A and D of the Beaufort Gyre Exploration Project (BGEP) will be extended through the 2015 season. The deployments are at 75°N, 150°W and 74°N, 140°W, respectively, and began in 2012 and 2013. The AWAC measurements can be used to estimate directional wave spectra every hour during open water periods, as well as ice draft during ice-covered periods.

Table 3: Sea State DRI observational assets

Platform	Topic	Investigator(s)	Measurements
R/V *Sikuliaq*	Atmosphere	Guest and Fairall	Ship basic meteorological stations; weather observations; upper-air (rawinsondes, balloons and tethered kit); turbulent fluxes; radiation; surface temperature; clouds
R/V *Sikuliaq*	Sea ice; waves in ice	Ackley, Weissling, Maksym, Doble, and Wadhams	Ice coring; shipboard digital photography; UAV photography; underway ice thickness (EMI); ice surface elevation (ship-based and terrestrial LIDAR); AUV under-ice swath for ITD and FSD; AUV ADCP for waves; pancake sampler; waves-in-ice buoys
R/V *Sikuliaq*	Upper-ocean physics	Stammerjohn, Maksym, and *Winsor	Towed CTD and EcoPuck (chl a, turbidity, CDOM) (Acrobat); Ship CTD casts, two-ship ADCPs (high-resolution and hull-mounted); AUV CTD and ADCP; 3 gliders w/ CTD and EcoPuck
R/V *Sikuliaq*	Large-scale ocean circulation	Stammerjohn and *Winsor	CTD profiling; underway CO_2 and TSG
R/V *Sikuliaq*	Sea state	Graber, Thomson, Guest, and Fairall	Marine radar; 2 shipboard video systems for wave breaking area estimates; downlooking LIDAR
Remote sensing	Sea ice; waves; waves in ice	Gemmerich, Lehner, and Holt IceBridge Science Team (sea ice)	TerraSAR-X Satellite; Satellite Active and Passive Microwave, Airborne Lidar Elevation and digital photography (NASA IceBridge Aircraft)
Autonomous buoys	Sea ice	Maksym, Stammerjohn, Ackley, Doble, Wadhams, ^Perovich, and ^Rigor	Ice growth, drift, and deformation; ice temperature profiles (ice mass balance buoys and GPS position buoys); surface TP (SVP); waves-in-ice buoys
Autonomous Buoys	Sea state, waves, atmosphere, upper ocean	Thomson, Doble, Wadhams, Maksym, ^Steele, and ^Rigor	Sea state and turbulent flux (SWIFT) buoys, wave buoys; surface TP (SVP), upper ocean (UpTempO buoys)
Moorings	Sea state, ice	Thomson	2 acoustic wave and current profilers (AWACs) (continuation of MIZ DRI deployments)

* Guest Investigators; ^ Buoy Providers (external to DRI)

Table 4: Sea State DRI buoys

Type	Quantity	Measurements	Investigator(s)
Sea State/Flux (SWIFT) Buoys	4	Sea state, atmospheric turbulent fluxes, SST	Thomson
Wave Buoys	10	Waves, amplitude, directional wave spectra (5 MIZ buoys, 5 new)	Doble and Wadhams
SAMS/WHOI Ice Mass Balance and GPS	5	Ice temperature profiles, ice thickness, snow depth, SST, SAT	Maksym
WHOI AWS (in ice)	1	Surface air temperature, pressure, winds, relative humidity	Maksym
CRREL Ice Mass Balance Buoys	2	Ice temperature profiles, snow depth, ice thickness, ocean T and S, pressure (floe isostasy), atmospheric pressure, SAT	Ackley and ^Perovich
UW UpTempo	3	Upper ocean temperature (50 m), conductivity (2 levels)	^Steele and Stammerjohn
UW SVP	3 to 6	Surface temperature and pressure, position (ice drift)	^Rigor and Stammerjohn

^Buoy Suppliers (External to DRI)

4.3 Modeling

We will consider modeling from a spectral perspective, i.e., by means of third generation models such as WW3 and 3GWAM used for operational forecasting, but also employ in parallel the phase-resolving models discussed earlier, built on the undergirding fundamental equations — especially in consideration of the directional wave evolution experiments. The latter will be used contemporaneously to explore the physics of wave–ice interactions and to develop parameterizations suitable for the spectral models, depending on ice properties available in near real time.

Recall that dissipation of wave energy, changes to the 'effective' wavenumber of the waves in the ice field, i.e., dispersion, and scattering are the main wave–ice interactions in the context of spectral modelling. (We use the word 'effective' to represent a composite wavenumber that coalesces dispersion in the ice–water matrix, as clearly the wavenumber in the water between ice floes is the same as in the open sea unless frazil ice is present in the leads and polynyas.) The first two effects can be accommodated in a new S_{id} ('ice dissipation') term, which passes information about wavenumber/group velocity to the advection term at each integration step. The third effect is included in a separate conservative S_{is} 'ice-scattering' term that captures spatial adjustments of the directional spread and wave amplitude in the penetrating wave spectrum, including attenuation, without depleting the mean wave energy. S_{id} and S_{is} combine to make up the S_{ice} in Eqn. 1. Observe, however, that 2D wave scattering within the ice field alone will not be perfectly conservative because the field of randomly distributed and randomly sized ice floes is not of infinite extent. Localization effects arise because of interference, which the phase-resolving models compute precisely by keeping track of coherence, and a reduction in wave amplitude with penetration into the ice occurs that is balanced by an accrual of wave trains liberated into the open ocean. So, when the MIZ and the contiguous open sea are consolidated, wave scattering is conservative but it is not within the ice field alone (irrespective of any dissipation). As a result, if S_{is} is used, the term must conjoin influences from the sea ice and the neighboring ocean or risk being a poor approximation to the physics of ocean wave propagation in an ice field, which it is necessary to quantify by means of a fully phase-resolving 2D scattering theory.

4.3.1 Phase-averaged spectral models for wave–ice forecasts

During the 1970s and 80s, phase-averaged finite difference wave models were widely adopted for wave hindcasting and forecasting, based on wave energy or wave action conservation equations such as Eqn. 1 (Clancy et al., 1986; SWAMP, 1985). This advance liberated the wave modeler from reliance on grossly unsatisfactory assumptions about the wave state (e.g., full development or fetch limited) and the forcing (e.g., winds that are steady and/or uniform

over a fetch) used in parametric models. Instead, the model numerically integrates the partial differential equation, simultaneously allowing for unsteady and non-uniform forcing, advection, highly nonlinear source terms (e.g., wave breaking), and treatment of swell. The most recent major advancement in this elegant mathematical treatment was the introduction of 3GWAM (Komen et al., 1984). WW3 (Tolman, 1991, 2009), used today for Navy operations, falls into this category, as does the WAM model (WAMDI Group, 1988; Komen et al., 1994) used at the ECMWF. While certain aspects of the 3GWAM have advanced rapidly in recent years (e.g., Tolman, 2003, 2008; Ardhuin et al., 2010), with similar advancement in applications (e.g., Janssen, 2008), the fundamentals are essentially unchanged from the 1980s. Although very powerful, the 3GWAM approach has definite limits. First, the discretized treatment of spatial variability implies dependence on geographic resolution. This presents a number of challenges for the modeler to handle (or errors to accept) but perhaps most relevant to arctic applications is in the context of model inputs. Even if given a perfectly detailed description of the sea ice, a wave modeler still must represent the sea ice using some representative quantities for each grid cell. Spatial averaging is the most obvious approach, although one can imagine using a statistical representation as input, e.g., a FSD. Regardless, sub-grid-scale processes must be parameterized, which is a challenge when modeling the notoriously heterogeneous ice cover of the MIZ.

The second definite limit of the 3GWAM is similarly obvious; the model is incapable of revealing fundamental truths about the real ocean that were not already understood by the model designer. If the science underpinning a source term paramerization is vague or speculative, the model predictions will similarly be vague and speculative. This implies that model results must be interpreted in context with these uncertainties and, further, that the wave model developers must work diligently to incorporate the most realistic physics that present knowledge allows. Advancing this knowledge of wave physics is, of course, a major goal of this DRI, as well as the downstream goal: implementation in the model. Here, we briefly review plans for

- implementation of new physics in spectral wave models
- maximizing benefit to wave model development from other DRI efforts (and vice versa)
- model applications for demonstration and validation

In the real ocean, the effect of sea ice on waves can be split into two categories: 1) scattering, which is energy-conserving and we have denoted by S_{is} and 2) various non-conservative (dissipation) processes that we designate collectively as S_{id}. Implementation in the 3GWAMs will follow this categorization. In principle, any number of non-conservative terms can be included simultaneously, provided that they represent unique physical processes, e.g., turbulence at the ice–water interface versus quasi-continuous frazil ice represented as a viscous

layer. As noted above, we will endeavor to avoid a particular mistake of the 3GWAM's past: aggregating such unique physical processes into parameterized 'catch-all' terms, for example, we will not use a viscoelastic source term to accommodate what we believe is reflection. We anticipate that our representations will evolve toward greater sophistication in this regard during the project. For example, for the S_{id} term, a simple parameterization strategy of treating all ice types using a viscoelastic layer (with, of course, nonstationary and nonuniform effective viscosity and elasticity) may be used initially as the sole S_{id}. Later, the viscoelastic parameterization might be used to represent only frazil and pancake ice, while a further separate S_{id} term would be employed to represent losses associated with collisions between floes.

With 3GWAM physics development, for each given physics routine, a conventional methodology will be followed. The code is first verified against simple external calculations to detect and eliminate coding errors. Sensitivity to input parameters is tested and documented. Then, the routines are applied in realistic hindcasts for which observations are available. In the context of the DRI, the primary validation dataset will be the 2015 field experiment, though we expect to also benefit from the field measurements made under the MIZ DRI (summer 2014).

Both terms, S_{is} and S_{id}, will be nonstationary, nonuniform, and frequency-dependent as appropriate. In both cases, three strategies are possible: 1) for the model to read in ice-related parameters and calculate the physics internally; 2) for the model to rely on pre-computed physics, reading in the physical response (attenuation rate, for example); and 3) some hybrid approach, e.g., the model reads in ice-related parameters and calculates the physical response using a lookup table or parametric fitting based on pre-computed physics.

The conservative term, S_{is}, will be implemented as diffuse reflection (i.e., 'ice scattering') controlled by two parameters, one associated with the percent reflection and another controlling the strength of diffusion in directional space. Both parameters must be scaled such that they are convergent (i.e., without incorrect dependence on resolution). This implementation will present no major challenge. The greater challenge is to determine the appropriate coefficients. It is acknowledged that the physical process that causes reflection will be different for different types of ice cover, e.g., reflection from leads and keels in continuous ice versus reflection from distinct ice floes in the MIZ. We envision this being handled in a single routine with multiple, separate processes. Although conservative, scattering should be expected to modify dissipation, and the entire system interacts in a nonlinear way. The governing equation of 3GWAMs allows treatment of such nonlinearity, albeit with the aforementioned limitations associated with resolution and fidelity of the physics.

In the absence of ice cover, the relation between wavenumber k_r and wave frequency is traditionally calculated using the linear dispersion relation in 3GWAMs. In a number of

theoretical derivations of the non-conservative term S_{id} (Liu and Mollo-Christensen, 1988; Keller, 1998; Wang and Shen, 2010), the problem is presented as a solution of a modified dispersion relation in which the wavenumber is complex $k = k_r + ik_i$. This is related to the source term in a very simple way. The energy dissipation rate $D = -2c_g k_i = S_{\mathrm{id}}/E$. The real part of the wavenumber solved in this fashion is different than that from linear wave theory in the presence of sea ice, but should converge to that value as the ice cover approaches zero. This modified real wavenumber, and corresponding group velocity and phase velocity, produces an effect analogous to refraction and shoaling by bathymetry. The process will be implemented and tested in the 3GWAMs. As mentioned above, we will allow for multiple simultaneous routines for the non-conservative term S_{id}. The dissipation rates will be treated in an additive way, analogous to how swell dissipation and whitecapping dissipation are treated in an additive way presently. However, only one dispersion relation can be used for the purpose of calculating the real part of the wavenumber. This can be implemented such that the most appropriate routine is selected based on the type of ice cover at a particular grid cell. While we acknowledge that it would be best to use a unified dispersion relation that accommodates every imaginable effect of ice on wavenumber simultaneously, we feel this is impractical.

The phase-averaged modeling components of the DRI are heavily dependent on other components. Theoretical modeling components will provide software to implement as routines in WW3 (this process has already started) and will provide guidance on selection of input variables. For example, the Wang and Shen model requires specification of effective viscosity and modulus of elasticity. These are obviously not variables produced by operational ice models, nor are they variables that can be derived from observations in a straightforward way. Connecting such variables to observable quantities such as ice concentration, FSD, ice thickness, and snow thickness is a major challenge, but necessary for the 3GWAMs. Guidance from the discrete ice floe model and phase resolving wave model components of the DRI are similarly essential during development of the phase-averaged models. Without this contribution, the latter is an unsatisfactory mixture of theory and guesswork. Observations from ship, buoy, aircraft, and satellite will also be used to calibrate or verify, as appropriate. The observations will be especially useful to determine the relative magnitude of S_{is} versus S_{id}. Both terms have a similar role, in the sense of attenuating swell along a transect that enters the MIZ, but only one will result in reflected waves that can be measured. The relative magnitude of these terms is not known a priori and certainly this will not be a fixed relation but will vary according to local conditions.

We will utilize satellite, airborne, and in situ wave observations to invert for necessary parameters (e.g., effective viscosity) using selected mathematical models and WW3 hindcasting for the DRI region. These parameters will be compared with observed rheology (similar to

Rogers and Holland, 2009), improving our understanding of quantitative relations between mathematical modeling constructs versus observable sea ice conditions. Although the 3GWAM models will be unable to use FSD directly, we anticipate that satellite observations of FSD will have an essential role in characterizing observed wave response and in relating it to the model physics.

While the focus of the DRI is on the Beaufort and Chukchi seas, which are not exposed to swells from the open ocean, we will use remote sensing and modeling to study exposed areas of the Arctic, viz. near the Nordic Seas. Remote sensing observations of temporal variations in the MIZ geographic extent and FSD will be used with wave information (model and satellite) to connect wave events with seasonal ice breakup events. Using the wave model, it is relatively straightforward to identify the sources of observed swells.

We also anticipate that in situ measurements of momentum and energy fluxes will provide a better handle on the behavior of the 'open water' source terms under partial ice cover. The obvious approach for the modeling is to reduce these terms in proportion to ice coverage, but this must be verified. It is acknowledged that detangling the contributions from multiple quantities (scattering by ice, attenuation by ice, ice-modified attenuation by whitecapping, and ice-modified atmosphere-to-wave energy flux) when interpreting the observations will be a significant challenge.

4.3.2 Phase-resolving models for wave–ice interactions

Ideally, the full set of ice variables necessary would include ice concentration and thickness and FSD. In reality, only the concentration is available operationally at this time from the satellite-based SSMIS measurements, although FSD and proxies for ice thickness can be obtained from intensive field campaigns. Unfortunately, ice concentration alone cannot unambiguously describe the physics of wave–ice interactions needed to estimate the properties of waves propagating through sea ice fields. Therefore, the phase-resolving models, analyses of literature and existing datasets, results of new laboratory tests, field observations, and remote sensing data products, as they become available, will be used to develop ensembles of possible scenarios for a set of coverage conditions ranging from 0% (open ocean) to 100% (solid ice). Parametric semi-empirical relationships and look-up tables, which are necessary for the spectral modeling based on ice-coverage alone, may potentially then be developed as the best-guess/most-likely outputs of the ensemble set. Separate parameterizations will be sought for conditions of partial ice coverage and solid ice. The threshold needs to be set on what is regarded as solid ice in terms of ice coverage. At this stage, 0.9 concentration appears a reasonable threshold.

Several theories for wave–ice interactions exist in the literature, but it appears that two classes can be used to build a general framework: viscoelastic theory, where the entire ice

cover is regarded as a continuum, and scattering theory, which accumulates the effect of multiple reflections from the many ice floes of different sizes that constitute the MIZ. There is no doubt that there are considerable advantages to being able to represent the ice cover as a continuum, but the current viscoelastic model (Wang and Shen, 2010, 2011) assumes the ice cover is uniform, i.e., the model's viscoelastic moduli are constant. Consequently, there remain two challenges: 1) developing a second generation viscoelastic formulation that allows for variable moduli to be prescribed, which is very difficult, or using a discretized continuum that matches the waves as they propagate through a set of strips with different moduli; and 2) finding a way to relate the in situ sea ice morphology to the viscoelastic moduli. For the latter a synthesized approach could be used, where scattering theory calibrates a viscoelastic parameterization that is potentially more amenable to being absorbed into a wave model.

4.3.3 Coupling and integration of models

As waves propagate into a large ice sheet, they may break the sea ice causing cracks and leads, and, potentially, they can even help to build pressure ridges given enough time. In broken MIZ sea ice, they define and progressively modify the FSD through breakage. They also impact on the local circulation, which can change the ice concentration. As a result, the wave–ice interaction regime and the respective parameterizations to be employed need to change. Once the sea ice is broken, the effective wave fetch adapts as the waves in the ice become subject to wind forcing. Consequently, the coupling arising from wave–ice interactions is vitally important to wave forecasting in polar seas. As noted, the energy, momentum, heat, and mass exchanges are perturbed when waves are present, the surface roughness and water drag change, and formation of new ice is affected. Initially these basic processes for operational wave forecasts will be parameterized with a simple wave–ice coupling module within WW3 and 3GWAM, with the goal of improving the model in due course.

In the context of the viscoelastic mechanism of wave–ice interaction or, indeed, modern scattering paradigms such as effective media theory with its associated coherent potential approximation [e.g., Dixon and Squire (2001) discuss the application of this theory to sea ice], an effective viscosity emerges that defines the dissipation and an effective modulus of elasticity that can be used to estimate how the real part of the wavenumber $k = k_r + ik_i$ changes in space and time. These quantities are now spatially variable and will also change in time as the sea ice cover evolves. Directional/frequency scattering will be parameterized by means of laboratory experiments and 2D surface modeling of waves in ice fields. As the additional theories are incorporated, they may need to be parameterized in terms of the supplementary energy source/sink terms to allow us to have separate formulations for different mechanisms and to have some mechanisms switched off (for example, floe–floe collisions in solid ice will be much less substantial) while others remain active. This is important because the severity

of each process in comparison with others varies across the ice field and for different ice fields. We should try to avoid the previous disadvantages of wave modeling when different physics, e.g., for whitecapping and swell dissipation, was amalgamated as a single wave dissipation source function, which was then describing neither physics adequately and was subject to re-tuning for particular circumstances rather than incremental improvement in performance as understanding of the physics advanced.

Acknowledging the difficulties and uncertainties associated with simultaneous inclusion of conservative and non-conservative processes in a model, the spectral wave–ice models built on physical principles will allow incremental improvements as new physics and new data become available. Operationally, the most important step would be the availability of ice thickness information and FSD. These would allow us to use unambiguous parameterizations instead of the most likely scenarios and lookup tables. On another level of practical applications, observation-based validation and calibration of existing theories is needed. The complex nature of wave–ice interactions may require additional mechanisms to be incorporated. This can be done by means of separate source terms in the spectral models, which may or may not be coupled with existing source functions. Finally, the full coupling of wave and ice models will need to be developed. For the same initial dynamic conditions, e.g., a wave spectrum, wind speed and FSD, the temperature regime may cause healing/melting of the ice and therefore different consequences for the wave modeling outputs.

The viscoelastic model of Wang and Shen (2010) implemented in WW3 is linear in its most obvious application. However, as our knowledge of the nonlinear aspects of wave–ice interaction advances, this can easily be incorporated into the existing model. For example, the effective viscosity and modulus of elasticity parameters can be a function of a variable derived from the wave model spectrum, the mean square slope. The resulting nonlinear source term is readily accommodated by the governing equation of the 3GWAMs.

In parallel, the NERSC WIFAR ice–ocean model, based upon TOPAZ driven by ECMWF atmospheric fields and 3GWAM, and built for the Fram Strait region of the Greenland Sea (Squire et al., 2013; Williams et al., 2013a,b), will be further developed for the Arctic Basin. This will allow phase-resolving wave models to be used directly through lookup tables with less parameterization, and offers an independent calibration of the envisioned spectral model.

In the context of Navy operational modeling, the overall goal is to have the Navy's wave model (presently WW3) fully coupled with the Navy's ice model ['Los Alamos Community Ice CodE', CICE; Hunke et al. (2008)] such that the effect of ice on waves is calculated in the wave model and the reverse is calculated in the ice model. Because the DRI is focused on science rather than operational transition, the actual modeling platform becomes secondary. For example, development within the general WAM framework is satisfactory because methods should be transferable to WW3. One DRI component involves application of the CICE model

(implying one-way coupling), but none include development of CICE nor incorporation of CICE in a two-way coupled system. We anticipate that some methods developed within other models, e.g., WIFAR, could be transferred to CICE; this would have to be done external to the DRI. However, we recognize that the two-way coupling between waves and ice is a critically important feature of the real MIZ, e.g., as observed by Doble and Bidlot (2013), and thus should not be wholly excluded from 3GWAM efforts of the DRI. To this end, we will implement in the wave models simple routines to account for the fracturing and healing of the ice. While being an interim and insufficient solution (e.g., advection of ice would not be represented), it will allow us to reproduce in the 3GWAM modeling some fundamental behaviors observed in the real ocean.

Modeling applications will focus on the 2015 field campaign. During late winter and spring of 2015, wave hindcasts will be produced for autumn 2014 that can be used to finalize the field plans. Preliminary hindcasts will be performed using archived winds and ice (similar to what is shown in Figure 2). Final hindcasts will be produced using the Earth System Modeling Framework, with coupling between waves, ice, ocean, and atmosphere (one-way coupling in the context of waves–ice, two-way coupling otherwise). Results will be analyzed for the purpose of planning the cruise for autumn 2015, and will be verified against available remote sensing data. During the field campaign, ice and ocean forecasts will be available from the Navy's Arctic Cap model [4], and wave forecasts will similarly be available from operational centers (Naval Oceanographic Office and ECMWF). After the field campaign, hindcasts will be used with the observations to develop, calibrate, and verify new physics, and to assist in interpretation of observations (models being especially useful for filling in gaps where observations are not available).

4.4 Laboratory experiments

While not part of the original DRI there are advantages to collecting experimental data in the laboratory, should the opportunity arise. Dedicated laboratory measurements of waves in the presence of ice are rare due to apparent logistical difficulties. Recently Montiel et al. (2013a,b) investigated how compliant disks behave in a wave field, and there are a number of earlier studies by Wadhams, Martin, Sakai, Shen, and others. Such experiments are generally hard to scale, because the 'sea ice' (which may be synthetic) needs to flex as well as execute its translational and rotational motions. Also, laboratory experiments often concentrate exclusively on properties of ice disturbed by the waves rather than on wave dynamics influenced by the ice (Wang and Shen, 2010; Naumann et al., 2012; De la Rosa and Maus, 2012). However, laboratory experiments are helpful in establishing enhancements

[4] `http://www7320.nrlssc.navy.mil/hycomARC/prologue.html`

to standard linear theories such as energy lost to turbulence or collisions, or how different classes of sea ice, e.g., pancake ice or frazil, react to a wave field. The opportunity to use HSVA (Hamburg Ship Model Basin), in particular, should be taken if funds permit.

Meylan is pursuing a series of laboratory experiments to test various mechanisms for wave energy dissipation. It is anticipated that these will provide a useful guide to the modeling and could also be helpful in the interpretation of the experimental results.

5 Relevant Ongoing Programs

There are several ongoing efforts that complement the work planned in the Sea State DRI. As relevant programs are identified, representatives will be invited to Sea State DRI meetings, and opportunities for scientific collaboration as well as logistic resource sharing will be explored.

As the primary example, the Marginal Ice Zone DRI is ongoing and will conduct a field experiment surrounding the ice breakup in the Beaufort Sea during the summer of 2014. Some buoys and moorings will remain deployed through the Sea State DRI experiment in 2015, thus creating a much longer time series. The MIZ DRI focus on ice breakup is a logical complement to the Sea State DRI focus on freeze-up. Many of the wave–ice physics studied will be in common between the DRIs; the preconditioning of the arctic system, however, will be very different, both from breakup to freeze-up and from year to year.

Many NSF-funded projects are relevant to the Sea State DRI. The BGEP moorings are already supporting AWAC instruments for the DRI. Other moorings, such as those by M. Alford (APL-UW) and J. Mackinnon (SIO-UCSD), may complement the DRI. Guest investigators to the DRI might supplement the instrumentation available to the DRI (e.g., UpTemp-O buoys from M. Steele at APL-UW or gliders from P. Winsor at UAF), or provide data delivery systems (e.g., the International Arctic Buoy Programme by I. Rigor at APL-UW).

The NOPP Waves program dedicated to updating the physics of the WW3 model is a related initiative. Within this program, several teams are working on updating input, dissipation, nonlinear interaction, and shallow water terms of WW3 (but not wave–ice physics). Collaboration with the NOPP teams would allow the Sea State DRI to benefit both from using the most up-to-date versions of WW3 and, once the wave–ice scattering and dissipation terms are ready, from extensive testing and calibrating of WW3, which is currently being undertaken within NOPP.

Finally, NASA Ice Bridge aerial surveys during the winter and early spring will be used to understand the preconditioning of the ice cover and the large-scale context of an incremental climatology.

6 Data Policy

The following data policy derives from experience in multiple ONR DRIs. Successful DRIs share a distinguishing characteristic: tightly integrated experimental and numerical efforts followed by highly collaborative analysis efforts. This is essentially the difference between a single, large, coordinated experiment and a large collection of independent projects working in parallel. To function well, the single, large, coordinated experiment requires open data sharing. Moreover, rapid, open data release is becoming standard for large programs. The Sea State DRI data policy recognizes this and attempts to strike a balance with rapid, full release within the Sea State DRI team followed by public release at the conclusion of the program. The Sea State DRI consists of all investigators participating in the integrated efforts associated with the DRI. This includes the core team of ONR-supported investigators funded directly by the DRI and investigators funded via other mechanisms, but coordinated as part of the Sea State DRI. Data will include observations from field programs, remote sensing data, and model results, all of which will be treated equally for the purposes of the program data policy. All data are collected for basic research, and will be unclassified. As the Sea State DRI also represents an ONR contribution to the U.S. inter-agency Study of Environmental Arctic Change (SEARCH), data will also be released to an appropriate data management facility for archiving, dissemination, and curation. Given the complex nature of the science questions and challenges associated with collecting the necessary observations, the success of the Sea State DRI depends on open, effective data sharing and collaboration. To facilitate sharing of data and collaboration among DRI scientists, the DRI will establish a program data archive accessible via the DRI website[5]. To further promote and support sharing and collaboration, the Sea State DRI specifies the following policies to govern the use of data collected under the program.

6.1 Data use

It is not ethical to publish data without proper attribution or co-authorship. The data are the intellectual property of the collecting investigator(s). The intellectual investment and time committed to the collection of a data set entitles the investigator to the fundamental benefits of the data set. Publication of descriptive or interpretive results derived immediately and directly from the data is the privilege and responsibility of the investigators who collect the data. There are two possible actions for any person making substantial use of Sea State DRI data sets, both of which require discussion with and permission from the data collector:

1. Expectation of co-authorship. This is the usual condition. Scientists making use of the

[5] `http://www.apl.washington.edu/project/project.php?id=arctic_sea_state`

data should anticipate that the data collectors would be active participants and require co-authorship of published results.

2. Citation and acknowledgement. In cases where the data collector acknowledges the importance of the application but expects to make no time investment or intellectual contribution to the published work, the data collector may agree to provide the data to another scientist, providing data reports are properly cited and the contribution is recognized in the text and acknowledgments.

Authors must share and discuss manuscripts with all Sea State DRI investigators who contributed data prior to submission anywhere. Agreements about publication, authorship, or citation should be documented at a minimum by e-mail among the investigators.

6.2 Roles and responsibilities

Principal Investigators who are responsible for the collection of observational data or generation of model output during the Sea State DRI are considered participating scientists and may request data from and provide data to other participating scientists. Participating scientists have primary responsibility for quality control of their own data and making them available in a timely fashion to the rest of the Sea State DRI participating scientists. Data should be released as soon as possible, through the Sea State DRI data archive, along with full metadata and supporting documentation that can be used by other researchers to judge data quality and potential usefulness. The data contained in the archive are made available even though they may not be "final" (i.e., error-free) data. Consequently, it is the responsibility of the user to verify the status of the data and to be aware of its potential limitations. Participating scientists who wish to use someone else's data sets are responsible for notifying those Principal Investigators of their intent and inviting collaboration and/or co-authorship of published results. Participating scientists must consider the interests of graduate students and post-docs before publishing data. Plans for graduate student and post-doc projects must be discussed openly and every effort made by all Sea State DRI investigators to facilitate and protect these efforts. For the duration of the Sea State DRI (2013-2017), data will be restricted to Sea State DRI investigators. Dissemination beyond program investigators will require the agreement of Sea State DRI investigators and the cognizant ONR program officers. After this time, Sea State DRI participating investigators are required to submit their data to the official data management facility for public dissemination and long-term curation. The Sea State DRI prohibits third party data dissemination; participants are not allowed to redistribute data taken by other Sea State investigators. All potential users who access the data will be reminded of the Sea State DRI commitment to the principle that data are the

intellectual property of the collecting scientists. Program sponsors of participating scientists may arbitrate and reach agreement on data sharing questions when they arise.

7 Abbreviations/Glossary

AUV	autonomous underwater vehicle
AWAC	acoustic wave and current meter
AWS	autonomous weather station
DRI	Department Research Initiative
ECMWF	European Centre for Medium-Range Weather Forecasts
EMI	electromagnetic induction (shipboard ice thickness measurement)
FSD	floe size distribution
HSVA	Hamburg Ship Model Basin
IMB	ice-mass balance buoy
ITD	ice thickness distribution
3GWAM	3rd Generation WAve prediction Model
LIDAR	light detection and ranging
MIZ	marginal ice zone
NERSC	Nansen Environmental and Remote Sensing Center
NSIDC	National Snow and Ice Data Center
ONR	Office of Naval Research
SAR	synthetic aperture radar
SSMIS	special sensor microwave imager/sounder (for ice mapping)
SWIFT	surface wave instrument float with tracking
TOPAZ	(Towards) an Operational Prediction system for the North Atlantic European coastal Zones
UAV	unmanned aerial vehicle
WIFAR	Waves-in-Ice Forecasting for Arctic Operators
WW3	WAVEWATCH III wave model

8 References

Ackley, S. F., and others, 2002. Wave–ice interaction during ice growth: The formation of pancake ice. Proceedings of the 16th IAHR Ice Symposium, Dunedin, New Zealand, Dec. 12–16, 2002, 158–164.

Anderson, R. J., 1987. Wind stress measurements over rough ice during the 1984 Marginal Ice Zone Experiment. J. Geophys. Res., 92, 6933–6941.

Andreas E. L., and others, 2010a. Parameterising turbulent exchange over summer sea ice and the marginal ice zone. Quart. J. Roy. Meteor. Soc., 136, 927–943, doi:10.1002/qj.618.

Andreas E. L., and others, 2010b. Parameterizing turbulent exchange over sea ice in winter. J. Hydrometeor., 11, 87–104, doi:10.1175/2009JHM1102.1.

Andreas, E. L., W. B. Tucker III, and S. F. Ackley, 1984. Atmospheric boundary-layer modification, drag coefficient, and surface heat flux in the Antarctic marginal ice zone. J. Geophys. Res., 89, 649–661.

Ardhuin, F., and others, 2010. Semiempirical dissipation source functions for ocean waves. Part I: Definition, calibration, and validation. J. Phys. Oceanogr., 40, 1917–1941.

Arrigo, K. R., van Dijken, G. L., 2011. Secular trends in Arctic Ocean net primary production. J. Geophys. Res., 116, doi:10.1029/2011JC007151.

Arrigo, K. R., and others, 2012. Massive phytoplankton blooms under Arctic sea ice. Science, 336 (6087), 1408, doi:10.1126/science.1215065.

Asplin, M. G., and others, 2012. Fracture of summer perennial sea ice by ocean swell as a result of Arctic storms. J. Geophys. Res., 117, doi:10.1029/2011JC007221.

Babanin, A. V., 2011. Breaking and Dissipation of Ocean Surface Waves. Cambridge University Press, 480p.

Barber, D. G., and others, 2009. Perennial pack ice in the southern Beaufort Sea was not as it appeared in the summer of 2009. Geophys. Res. Lett., 36, doi:10.1029/2009GL041434.

Bennetts, L. G., and others, 2010. A three-dimensional model of wave attenuation in the marginal ice zone. J. Geophys. Res., 115, doi:10.1029/2009JC005982.

Bennetts, L. G., V. A. Squire, 2009. Wave scattering by multiple rows of circular ice floes. J. Fluid Mech., 639, 213–238.

Bennetts, L. G., V. A. Squire, 2012a. On the calculation of an attenuation coefficient for transects of ice-covered ocean. Proc. R. Soc. Lond. A, 468 (2137), 136–162.

Bennetts, L. G., V. A. Squire, 2012b. Model sensitivity analysis of scattering-induced attenuation of ice-coupled waves. Ocean Model., 45–46, doi:10.1016/j.ocemod.2012.01.002.

Bennetts, L. G., T. D. Williams, 2010. Wave scattering by ice floes and polynyas of arbitrary shape. J. Fluid Mech., 662, 5–35, doi:10.1017/S0022112010004039.

Bidlot J.-R. 2012: Present status of wave forecasting at ECMWF. Proceeding from the ECMWF Workshop on Ocean Waves, 25–27 June 2012.

Birnbaum, G., C. Lpkes, 2002. A new parameterization of surface drag in the marginal sea ice zone. Tellus, 54A, 107–123.

Clancy, R. M., J. E. Kaitala, L. F. Zambresky, 1986. The Fleet Numerical Oceanography Center global spectral ocean wave model. Bull. Amer. Meteor. Soc., 67, 489–512.

De la Rosa, S., S. Maus, 2012. Laboratory study of frazil ice accumulation under wave conditions. The Cryosphere, 6, 729–741.

Dixon, T. W., V. A. Squire, 2001. Energy transport in the marginal ice zone. J. Geophys. Res., 106 (C9), 19,917–19,927.

Doble, M. J., J.-R. Bidlot, 2013. Wavebuoy measurements at the Antarctic sea ice edge compared with an enhanced ECMWF WAM: progress towards global waves-in-ice modeling. Ocean Model., 70, 166–173, doi:10.1016/j.ocemod.2013.05.012.

Dobrynin, M., J. Murawsky, S. Yang, 2012. Evolution of the global wind wave climate in CMIP5 experiments, Geophys. Res. Lett., 39, doi:10.1029/2012GL052843.

Donelan, M.A., and others, 2006. Wave follower measurements of the wind input spectral function. Part 2. Parameterization of the wind input. J. Phys. Oceanogr., 36 (8), 1672–1688.

Dozaki, M., T. Hayakawa, S. Sakai, 1999. Field observation on wave–ice interactions in the Okhotsk Sea, in Proceedings of the 9th International Offshore and Polar Engineering Conference, vol. 2, edited by J. S. Chung, pp. 628–635, International Society of Offshore and Polar Engineers, Cupertino, California.

Dumont, D., A. L. Kohout, L. Bertino, 2011a. A wave-based model for the marginal ice zone including a floe breaking parameterization. J. Geophys. Res., 116, doi:10.1029/2010JC006682.

Dumont, D., and others, 2011b. Forecasting waves-in-ice for Arctic operators. Oil Gas Rev., 9 (1), 18–20.

Fairall, C., and others, 2003. Bulk parameterization of air–sea fluxes: Updates and verification for the COARE algorithm. J. Climate, 16, 571–591.

Feltham, D. L., 2005. Granular flow in the marginal ice zone. Phil. Trans. R. Soc. Lond. A., 363, 1677–1700.

Filipot, J.-F., F. Ardhuin, A. V. Babanin, 2010. A unified deep-to-shallow-water spectral wave-breaking dissipation formulation. J. Geophys. Res., 115, doi:10.1029/2009JC005448.

Francis, J. A., and others, 2009. Winter Northern Hemisphere weather patterns remember summer Arctic sea-ice extent. Geophys. Res. Lett., 36, doi:10.1029/2009GL037274.

Francis, O. P., G. G. Panteleev, D. E. Atkinson, 2011. Ocean wave conditions in the Chukchi Sea from satellite and in situ observations. Geophys. Res. Lett., 38, doi:10.1029/2011GL049839.

Francis, J. A., S. J. Vavrus, 2012. Evidence linking Arctic amplification to extreme weather in mid-latitudes. Geophys. Res. Lett., 39, doi:10.1029/2012GL051000.

Gelci, R., D. H. Cazalé, J. Vassal, 1957. Prévision de la houle. La méthode des densités spectroangulaires. Bull. Infor. Comité Central Oceanogr. d'Etude Côtes, 9, 416.

Gemmrich, J., 2010. Strong turbulence in the wave crest region. J. Phys. Oceanogr., 40, 583–595.

Gemmrich, J., T. Mudge, V. Polonichko, 1994. On the energy input from wind to surface waves, J. Phys. Oceanogr., 24, 2413–2417.

Gemmrich, J. R., M. L. Banner, C. Garrett, 2008. Spectrally resolved energy dissipation rate and momentum flux of breaking waves, J. Phys. Oceanogr., 38, 1296–1312.

Gladstone, R. M., G. R. Bigg, K. W. Nicholls, 2001. Iceberg trajectory modeling and meltwater injection in the Southern Ocean. J. Geophys. Res., 106 (C9), 19,903–19,915.

Girard, L., D. Amitrano, J. Weiss, 2010. Failure as a critical phenomenon in a progressive damage model. J. Stat. Mech., P01013, doi:10.1088/1742-5468/2010/01/P01013.

Girard, L., and others, 2009. Evaluation of high-resolution sea ice models on the basis of statistical and scaling properties of Arctic sea ice drift and deformation. J. Geophys. Res., 114, doi:10.1029/2008JC005182.

Grebmeier, J. M., and others, 2006. A major ecosystem shift in the northern Bering Sea. Science, 311 (5766), 1461–1464, doi:10.1126/science.1121365.

Greenhill, A. G., 1887. Wave motion in hydrodynamics. Am. J. Math., 9, 62–112.

Guest, P. S., K. L. Davidson, 1987. The effect of observed ice conditions on the drag coefficient in the summer East Greenland Sea marginal ice zone. J. Geophys. Res., 92, 6943–6954.

Guest, P. S., K. L. Davidson, 1991a. The aerodynamic roughness of different types of sea ice. J. Geophys. Res., 96, 4709–4721.

Guest, P. S., J. W. Glendening, K. L Davidson, 1995. An observational and numerical study of wind stress variations within marginal ice zones. J. Geophys. Res., 100, 10,887–10,904.

Haas, C., 2012. Airborne Observations of the Distribution, Thickness, and Drift of Different Sea Ice Types and Extreme Ice Features in the Canadian Beaufort Sea. Offshore Technology Conference, 3–5 December 2012, Houston, TX, 8 pp.

Hasselmann, K., 1960. Grundgleichungen der Seegangsvorhersage. Schiffstechnik, 7, 191–195.

Herbers, T. H. C., and others, 2012. Observing ocean surface waves with GPS tracked buoys. J. Atmos. Ocean. Technol., 29, 944–959, doi:10.1175/JTECH-D-11-00128.1.

Herman, A., 2013. Numerical modeling of force and contact networks in fragmented sea ice. Ann. Glaciol. 54 (62), 114–120, doi:10.3189/2013AoG62A055.

Hibler, W. D., 1979. A dynamic thermodynamic sea ice model. J. Phys. Oceanogr., 9, 815–846.

Howells, 1960. The multiple scattering of waves by weak random irregularities in the medium. Phil. Trans. R. Soc. Lond. A, 252, 431-462.

Hunke, E. C., W. Lipscomb, 2008. CICE: The Los Alamos sea ice model, documentation and software user's manual, version 4.0. Tech. Rep. LA-CC-06-012, Los Alamos National Laboratory, Los Alamos, NM. (http://climate.lanl.gov/models/cice/index.htm).

Hunke, E. C., J. K. Dukowicz, 1997. An elastic-viscous-plastic model for sea ice dynamics. J. Phys. Oceanogr., 27, 1849–1867.

Iafrati, A., A. V. Babanin, M. Onorato, 2013. Modulational instability, wave breaking and formation of large scale dipoles. Phys. Rev. Lett., 110, 184504, doi:10.1103/PhysRevLett.110.184504.

Inoue, J., M. E. Hori, 2011. Arctic cyclogenesis at the marginal ice zone: A contributory mechanism for the temperature amplification? Geophys. Res. Lett., 38, doi:10.1029/2011GL047696.

Jackson, J. M., W. J. Williams, E. C. Carmack, 2012. Winter sea-ice melt in the Canada Basin, Arctic Ocean. Geophys. Res. Lett., 39, doi:10.1029/2011GL050219.

Janssen, P. A. E. M. 2008. Progress in ocean wave forecasting. J. Comp. Phys., 227(7), 3572–3594.

Keller, J. B., 1998. Gravity waves on ice-covered water, J. Geophys. Res., 103 (C4), 7663–7669.

Kohout, A. L., M. H. Meylan, 2008. An elastic plate model for wave attenuation and ice floe breaking in the marginal ice zone. J. Geophys. Res., 113, doi:10.1029/2007JC004434.

Komen, G. J., S. Hasselmann, K. Hasselmann, 1984. On the existence of a fully developed wind–sea spectrum. J. Phys. Oceanogr., 14, 1271–1285.

Komen, G. J., and others, 1994. Dynamics and Modelling of Ocean Waves. Cambridge Univ. Press, 532 pp.

Kwok, R., 2009. Thinning and volume loss of the Arctic Ocean sea ice cover: 2003–2008. J. Geophys. Res., 114, doi:10.1029/2009JC005312.

Kwok, R., G.F. Cunningham, 2008. ICESat over Arctic sea ice: Estimation of snow depth and ice thickness, J. Geophys. Res., 113, 1025-1030, doi:10.1029/2008JC004753.

Kwok, R., N. Untersteiner, 2011. The thinning of Arctic sea ice. Physics Today, 64, 36–41, doi:10.1063/1.3580491.

Lange, M. A., and others, 1989. Development of sea ice in the Weddell Sea, Antarctica. Ann. Glaciol., 12, 92–96.

Langhorne, P. J., and others, 2001. Lifetime estimation for a land-fast ice sheet subjected to ocean swell. Ann. Glaciol., 33, 333–338.

Lewis, M. J., and others, 2011. Sea ice and snow cover characteristics during the winter–spring transition in the Bellingshausen Sea: An overview of SIMBA 2007. Deep Sea Res. II, 58, 1019–1038.

Lindsay, R. W., J. Zhang, 2005. The thinning of Arctic sea ice, 1988–2003: Have we passed a tipping point? J. Climate, 18, 4879–4894.

Liu, A. K., B. Holt, P. W. Vachon, 1991. Wave propagation in the marginal ice zone: Model prediction and comparisons with buoy and synthetic aperture radar data. J. Geophys. Res., 96, 4605–4621.

Liu, A. K., P. W. Vachon, C. Y. Peng, 1991. Observation of wave refraction at an ice edge by synthetic aperture radar. J. Geophys. Res., 96, 4803–4808.

Liu, A. K., E. Mollo-Christensen, 1988. Wave propagation in a solid ice pack. J. Phys. Oceanogr., 18, 1702–1712.

Lytle, V. I., S. F. Ackley, 1996. Heat flux through sea ice in the western Weddell Sea: Convective and conductive transfer processes. J. Geophys. Res., 101, 8853–8868.

Markus, T., J. C. Stoeve, J. Miller, 2009. Recent changes in Arctic sea ice melt onset, freeze-up, and melt season length. J. Geophys. Res., 114, doi:10.1029/2009JC005436.

Masson, D., P. LeBlond, 1989. Spectral evolution of wind-generated surface gravity waves in a dispersed ice field. J. Fluid Mech., 202, 43-81, doi:10.1017/S0022112089001096.

Meier, W. N., D. Gallaher, G. G. Campbell, 2013. New estimates of Arctic and Antarctic sea ice extent during September 1964 from recovered Nimbus I satellite imagery. The Cryosphere, 7, 699–705, doi:10.5194/tc-7-699-2013.

Meylan, M., V. A. Squire, C. Fox, 1997. Toward realism in modelling ocean wave behaviour in marginal ice zones. J. Geophys. Res., 102 (C10), 22,981–22,991.

Meylan, M. H., D. Masson, 2006. A linear Boltzmann equation to model wave scattering in the marginal ice zone. Ocean Model., 11 (3–4), 417–427.

Montiel, F., and others, 2013. Hydroelastic response of floating elastic disks to regular waves. Part 1: Wave basin experiments. J. Fluid Mech., 723, 604–628.

Montiel, F., and others, 2013. Hydroelastic response of floating elastic disks to regular waves. Part 2: Modal analysis. J. Fluid Mech., 723, 629–652.

Naumann, A. K., and others, 2012. Laboratory study of initial sea-ice growth: Properties of grease ice and nilas. The Cryosphere, 6, 729–741.

Newyear, K., S. Martin, 1999. Comparison of laboratory data with a viscous two-layer model of wave propagation in grease ice. J. Geophys. Res., 104, 7837–7840, doi:10.1029/1999JC900002.

Overland, J. E., and others, 2012. The recent shift in early summer Arctic atmospheric circulation. Geophys. Res. Lett., 39, doi:10.1029/2012GL053268.

Overland, J. E., M. Wang, 2013. When will the summer Arctic be nearly sea ice free? Geophys. Res. Lett., 40, doi:10.1002/grl.50316.

Parkinson, C. L., J. C. Comiso, 2013. On the 2012 record low Arctic sea ice cover: Combined impact of preconditioning and an August storm. Geophys. Res. Lett., 40, 1356–1361, doi:10.1002/grl.50349.

Perovich, D. K., and others, 2007. Increasing solar heating of the Arctic Ocean and adjacent seas, 1979–2005: Attribution and role in the ice-albedo feedback. Geophys. Res. Lett., 34, doi:10.1029/2007GL031480.

Perrie, W., Y. Hu, 1996. Air-ice-ocean momentum exchange, part 1: Energy transfer between waves and ice floes. J. Phys. Oceanogr., 26 (9), 1705–1720.

Peter, M. A., M. H Meylan, Water-wave scattering by vast fields of bodies, SIAM J. Appl. Math. 70(5), 1567–1586.

Peters, A. S., 1950. The effect of a floating mat on water waves. Commun. Pure Appl. Math., 3, 319–354.

Polashenski, C., D. Perovich, Z. Courville, 2012. The mechanisms of sea ice melt pond formation and evolution. J. Geophys. Res., 117, doi:10.1029/2011JC007231.

Prinsenberg, S. J., I. K. Peterson, 2011. Observing regional-scale pack-ice decay processes with helicopter-borne sensors and moored upward-looking sonars. Ann. Glaciol., 52 (57), 35–42, doi:10.3189/172756411795931688.

Rampal, P., and others, 2008. Scaling properties of sea ice deformation from buoy dispersion analysis. J. Geophys. Res., 113, doi:10.1029/2007JC004143.

Rampal, P., J. Weiss, D. Marsan, 2009. Positive trend in the mean speed and deformation rate of Arctic sea ice, 1979–2007. J. Geophys. Res., 114, doi:10.1029/2008JC005066.

Rasmussen, E. A., P. S Guest, K. L. Davidson, 1997. Synoptic and mesoscale features over the ice-covered portion of the Fram Strait in spring. J. Geophys. Res., 102, 13,975–13,986.

Rogers, W. E., K. T. Holland, 2009: A study of dissipation of wind-waves by viscous mud at Cassino Beach, Brazil: Prediction and inversion. Cont. Shelf Res., 29, 676–690.

Rogers, W. E., M. D. Orzech, 2013. Implementation and testing of ice and mud source functions in WAVEWATCH III. NRL Memorandum Report, NRL/MR/7320–13-9462, 31 pp. (http://www7320.nrlssc.navy.mil/pubs.php)

Rogers, W. E., and others, 2011: On use of internal constraints in recently developed physics for wave models. Proc. 12th Int. Workshop on Wave Hindcasting and Forecasting and 3rd Coastal Hazards Symp., Big Island, Hawaii, October 30 – November 4, presentation slides.

Screen, J. A., I. Simmonds, 2010a. The central role of diminishing sea ice in recent Arctic temperature amplification. Nature, 464, 1334–1337, doi:10.1038/nature09051.

Screen, J. A., I. Simmonds, 2010b. Increasing fall-winter energy loss from the Arctic Ocean and its role in Arctic temperature amplification. Geophys. Res. Lett., 37, doi:10.1029/2010GL044136.

Screen, J. A., I. Simmonds, K. Keay, 2011. Dramatic inter-annual changes of perennial Arctic sea ice linked to abnormal summer storm activity. J. Geophys. Res., 116, D15105.

Serreze, M. C., and others, 1993. Characteristics of Arctic synoptic activity. Met. Atmos. Phys., 51, 147–164.

Serreze, M. C., A. H. Lynch, and M. P. Clark, 2001. The summer Arctic frontal zone as seen in the NCEP/NCAR reanalysis, J. Climate, 14, 1550–1567.

Shen, H. H., V. A. Squire, 1998. Wave damping in compact pancake ice fields due to interactions between ice cakes. In Antarctic Science Research Series, edited by M. O. Jeffries, 74, 325–342 (AGU, Washington, DC).

Shen, H. H., W. D. Hibler, M. Leppäranta, 1986. On applying granular flow theory to a deforming broken ice field. Acta Mech., 63, 143–160.

Shen, H. H., S. F. Ackley, M. A. Hopkins, 2001. A conceptual model for pancake-ice formation in a wave field. Ann. Glaciol., 33, 361–367.

Shen, H. H., B. Sankaran, 2004. Internal length and time scales in a simple shear granular flow. Phys. Rev. E, 70, 051308, doi:10.1103/PhysRevE.70.051308.

Showstack, R., 2013. Diminishing sea ice in the Arctic presents challenges and opportunities, Eos – Trans. Am. Geophys. U., 94 (31), 270–271.

Simmonds, I., I. Rudeva, 2012. The great Arctic cyclone of August 2012. Geophys. Res. Lett., 39, doi:10.1029/2012GL054259.

Simmonds, I., K. Keay, 2009. Extraordinary September Arctic sea ice reductions and their relationships with storm behavior over 1979–2008. Geophys. Res. Let., 36, doi:10.1029/2009GL039810.

Stammerjohn, S. E., and others, 2011. The influence of winds, sea-surface temperature and precipitation anomalies on Antarctic regional sea-ice conditions during IPY 2007. Deep Sea Res., II, 58, 999–1018.

Stammerjohn, S. E., and others, 2012. Regions of rapid sea ice change: An interhemispheric seasonal comparison. Geophys. Res. Lett., 39, doi:10.1029/2012GL050874.

Stroeve, J., and others, 2008. Arctic sea ice extent plummets in 2007. Eos – Trans. Am. Geophys. U., 89 (2), 13–14.

Stroeve, J. C., and others, 2005. Tracking the Arctic's shrinking ice cover: Another extreme September minimum in 2004. Geophys. Res. Let., 32, doi:10.1029/2004GL021810.

Squire, V. A., 1993. Ocean wave propagation in an ice field with varying concentration. In Proc. 3rd Int. Offshore Polar Conf., 2, ISOPE, Co, USA, 724.

Squire, V. A., S. C. Moore, 1980. Direct measurement of the attenuation of ocean waves by pack ice. Nature, 283, 365–368.

Squire, V. A., and others, 1995. Of ocean waves and sea ice. Annu. Rev. Fluid Mech., 27, 115–168.

Squire, V. A., 2007. Of ocean waves and sea-ice revisited. Cold Reg. Sci. Technol., 49 (2), 110–133.

Squire, V. A., G. L. Vaughan, L. G. Bennetts, 2009. Ocean surface wave evolvement in the Arctic Basin. Geophys. Res. Lett., 36, doi:10.1029/2009GL040676.

Squire, V. A., T. D. Williams, L. G. Bennetts, 2013. Better operational forecasting for contemporary Arctic via ocean wave integration. Int. J. Offshore Polar Eng., 23 (2), 81–88.

Steele, M., W. Ermold, J. Zhang, 2011. Modeling the formation and fate of the near-surface temperature maximum in the Canadian Basin of the Arctic Ocean. J. Geophys. Res., 116, doi:10.1029/2010JC006803.

Steele, M., J. H. Morison, N. Untersteiner, 1989. The partition of air-ice-ocean momentum exchange as a function of ice concentration, floe size, and draft. J. Geophys. Res., 94 (C9), 12,739–12,750.

Stephenson, S. R., L. C. Smit, J. A. Agnew, 2011. Divergent long-term trajectories of human access to the Arctic. Nature Climate Change, 1, 156–160.

SWAMP Group, 1985. Ocean Wave Modeling. Plenum Press, New York, 266 pp.

Terray, E., and others, 1996. Estimates of kinetic energy dissipation under breaking waves. J. Phys. Oceanogr., 26, 792–807.

Thomson, J., 2012. Wave breaking dissipation observed with SWIFT drifters. J. Atmos. Ocean. Tech., 29, 1866–1882, doi:10.1175/JTECH-D-12-00018.1.

Thomson, J., A. Jessup, J. Gemmrich, 2009. Energy dissipation and the spectral distribution of whitecaps. Geophys. Res. Lett., 36 (11), doi:10.1029/2009GL038201.

Tolman, H. L., 1991. A Third generation model for wind-waves on slowly varying, unsteady, and inhomogeneous depths and currents. J. Phys. Oceanogr., 21(6), 782–797.

Tolman, H. L. 2003. Treatment of unresolved islands and ice in wind wave models. Ocean Model., 5, 219–231.

Tolman, H. L. 2008. A mosaic approach to wind wave modeling. Ocean Model., 25, 35–47.

Tolman, H. L., 2009. User Manual and System Documentation of WAVEWATCH III® Version 3.14, Tech. Note, NOAA/NWS/NCEP/MMAB, 220 pp.

Tolman, H., D. Chalikov, 1994. Development of a third-generation ocean wave model at NOAA-NMC. In Proc. Waves Physical and Numerical Modeling, edited by M. Isaacson and M. C. Quick, 724–733 (Univ. of British Columbia Press).

Toyota, T., C. Haas, T. Tamura, 2011. Size distribution and shape properties of relatively small sea-ice floes in the Antarctic marginal ice zone in late winter. Deep Sea Res. II, 58 (9–10), 1182–1193.

Vagle, S., J. Gemmrich, H. Czerski, 2012. Effect of upper ocean stratification on turbulence and optically active bubbles. J. Geophys. Res., 117, doi:10.1029/2011JC007308.

Vaughan, G. L., L. G. Bennetts, V. A. Squire, 2009. The decay of flexural-gravity waves in long sea-ice transects. Proc. R. Soc. Lond. A, 465, 2785–2812.

Vaughan, G. L., V. A. Squire, 2011. Wave induced fracture probabilities for Arctic sea ice. Cold Reg. Sci. Technol. 67 (1–2), 31–36.

Vermaire, J. C., and others, 2013. Arctic climate warming and sea ice declines lead to increased storm surge activity. Geophys. Res. Lett., 40, 1386–1390, doi:10.1002/grl.50191.

Wadhams, P., 1973. The effect of a sea ice cover on ocean surface waves. PhD thesis, Univ. of Cambridge, England.

Wadhams, P., A. E. Gill, P. Linden, 1979. Transects by submarine of the East Greenland Polar Front. Deep-Sea Res. A, 26, 1311–1322.

Wadhams, P., and others, 1986. The effect of the marginal ice zone on the directional wave spectrum of the ocean. J. Phys. Oceanog., 16 (2), 358–376.

Wadhams, P., and others, 1988. The attenuation rates of ocean waves in the marginal ice zone. J. Geophys. Res., 93 (C6), 6799–6818.

Wadhams, P., and others, 2004. SAR imaging of wave dispersion in Antarctic pancake ice and its use in measuring ice thickness. Geophys. Res. Lett., 31, doi:10.1029/2004GL020340.

WAMDI Group, 1988. The WAM model – A third generation ocean wave prediction model. J. Phys. Oceanogr., 18, 1775–1810.

Wang, R., H. H. Shen, 2010. Gravity waves propagating into an ice-covered ocean: A viscoelastic model. J. Geophys. Res., 115, doi:10.1029/2009JC005591.

Wang, R., H. H. Shen, 2011. A continuum model for the linear wave propagation in ice-covered oceans: An approximate solution. Ocean Model., 38, 244–250.

Warren, S.G., and others, 1998. Snow depth on Arctic sea ice, J. Climate, 12, 1814–1829.

Weber, J. E., 1987. Wave attenuation and wave drift in the marginal ice zone. J. Phys. Oceanogr., 17, 2351–2361.

Williams, T. D., and others, 2013a. Wave-ice interactions in the marginal ice zone. Part 1: Theoretical foundations. Ocean Model., in press, doi:10.1016/j.ocemod.2013.05.010.

Williams, T. D., and others, 2013b. Wave-ice interactions in the marginal ice zone. Part 2: Numerical implementation and sensitivity studies along 1D transects of the ocean surface. Ocean Model., in press, doi:10.1016/j.ocemod.2013.05.011.

Winton, M., 2008. Sea ice – albedo feedback and nonlinear Arctic climate change. In Arctic Sea Ice Decline, 111–131(Washington DC, American Geophysical Union).

Young, I. R., 1999. Wind Generated Ocean Waves, Elsevier Ocean Engineering Book Series (Elsevier, New York).

Young, I. R., S. Zieger, A. V. Babanin, 2011. Global trends in wind speed and wave height. Science, 332 (6028), 451-455, doi:10.1126/science.1197219.

Zhang, J., and others, 2013. The impact of an intense summer cyclone on 2012 Arctic sea ice retreat. Geophys. Res. Lett., 40, 720–726, doi:10.1002/grl.50190.

Zhang, X., and others, 2004. Climatology and interannual variability of Arctic cyclone activity: 1948–2002. J. Climate, 17, 2300–2317.